Towards a better understanding of the ultimate behaviour of LWAC in compression and bending

Jan A. Øverli[a,1]

[a]Department of Structural Engineering, NTNU, Norwegian University of Science and Technology, NO-7491 Trondheim, Norway, E-mail: jan.overli@ntnu.no, Tel: +47 73594513

Abstract

There is a general scepticism regarding the use of lightweight aggregate concrete (LWAC) for structural applications. This concern is attached to the more brittle post-peak material behaviour and smoother crack surfaces of these concretes compared to normal density concrete (NWC). In this research, the post-peak material behaviour and the force transfer across cracks were considered to be unimportant, regardless of the weight of the concrete. The working hypothesis was that the three key material characteristics that generally dictate the ultimate response of concrete structures are: the large effect small secondary stresses have on compressive strength; the abrupt increase of transverse expansion at a stage close to, but not beyond, the peak stress level; and the rapid unloading of the material beyond the peak stress level. It follows from these features, that the strength, and especially the ductility, of structural concrete members depend on the local triaxial stress conditions that inevitably develop in the compressive zone just prior to failure, rather than on stress-redistributions due to post-peak material characteristics, as is commonly believed. In the verification process, results from experimental programmes reported in the literature were carefully examined using three-dimensional nonlinear finite element analysis. The somewhat lower ductility of LWAC members with decreasing density can be explained by a lower degree of stress triaxiality in the compressive zone compared to NWC. This seems to be a result of the often quite modest transverse expansion of LWAC concretes prior to failure and linked to a limited degree of microcracking within the material. Nevertheless, the load-carrying capacity of LWAC members is often similar to that of corresponding NWC members. The high strength-to-weight ratio of LWAC compared to conventional concrete means that increased use of the material would be both economical and environmentally friendly. A better understanding of the ultimate behaviour of LWAC in compression and bending can help increase the use of LWAC in structural applications.

[1] Corresponding author. Tel.: +47 73594513
E-mail address: jan.overli@ntnu.no

Keywords: Lightweight aggregate concrete, bending, shear, ductility, nonlinear analysis, triaxial stress

1 Introduction

Lightweight aggregate concrete (LWAC) has been used as a construction material for many decades, normally with the aim of reducing the dead weight of structures. This allows the dimensions of the foundations of buildings to be reduced in areas with low bearing capacities, inertia actions are reduced in seismic regions, and it is easier to handle and transport precast elements. In large and advanced structures, such as high-rise buildings, bridges and offshore structures, it has been applied with great success [1-5]. Yet, even with the major advantage of its reduced weight and high strength-to-weight ratio compared to conventional concrete, the use of LWAC is still limited as a mainstream construction material in the building industry.

The finite-element (FE) approach is a numerical method which can be used to assess the deformational and strength response for any geometry, boundary conditions and material during the entire loading history of a structure. It can be used in the design of new structures, especially those with complex geometries, or as an inexpensive alternative to experiments for the development of innovative and efficient building products and more accurate design rules, because it allows for a multitude of tests to be carried out numerically, with only a small number of laboratory tests needed to check the theoretical findings. These areas of application, however, have rarely been appreciated for concrete. The reason for this is at least two-fold. Firstly, concrete behaviour is often ‘tuned’ to specific types of structure, in which the material parameters must be ‘retuned’ depending on the problem type. Secondly, different analysts often obtain widely differing results when modelling the same structure using FE code due to the uncertainty connected with many of the material parameters going into the analysis [6-8]. This is awkward, since knowing the answer beforehand is almost a prerequisite for the success of the calculations. There are two main reasons for this lack of generality and objectivity when the FE method is applied to concrete structures. Firstly, the material models employed by many analysts do not realistically describe concrete as a material, and secondly, cracking of concrete can lead to numerical instabilities in the analysis if adequate precautions are not taken. In this respect, it is interesting to note that remarkably good numerical results have been reported when a brittle triaxial material model is used that takes into account the increased transverse expansion of the concrete prior to failure [9]. Unfortunately, anyone familiar with FE modelling of concrete structures knows that the common line of

action is to use uniaxial models in which the post-peak material behaviour is characterised by a gradual loss of load-carrying capacity. Moreover, when triaxial material data actually are implemented in these models, it is normally without a proper description of the abrupt transverse expansion of the concrete prior to failure, which is what actually gives rise to the triaxial stress conditions in the structure.

The majority of concrete researchers do not accept the assertion that concrete is a fully brittle material. Instead they rely heavily on the description of the post-peak behaviour of the concrete at the material level. In this respect, it is important to remember that the FE method works by breaking the structure into a finite number of elements, so that its overall deformational and strength response for arbitrary boundary conditions can be calculated through mathematical equations related to the behaviour of each individual element. What is needed, therefore, is a mathematical description of the response of a representative element of the material under well-defined states of stress. This means that the material data must have been established independent of any effects from the testing equipment. The neglect of this requirement is probably the main reason for the lack of a proper understanding of concrete at both the material and the structural level. If this is true, this must inevitably hamper the development of rational design rules and generally valid FE models for concrete. To make a leap forward in structural concrete research, it was therefore considered to be of crucial importance to first evaluate whether concrete really behaves as it is assumed to do, both as a material and in a structure.

Many consider the major disadvantage of LWAC to be its brittleness in compression at the material level compared to normal density concrete. The requirement of adequate strength, which can easily be fulfilled with lightweight concrete, is not the only design criterion, because adequate ductility is essential for safety in overload situations [10-13]. Ductility is of great importance in the redistribution of forces, and is also a major consideration in the design of structures in seismic areas. It is possible to achieve ductile structures by adjusting reinforcement ratios and proper detailing. However, some structures, e.g. large offshore shell concrete structures, are often heavily reinforced to satisfy other criteria than ultimate capacity. In such cases the brittle behaviour of concrete needs to be considered. The assumed limited post-peak behaviour of LWAC can help explain the limited use of the material, and requests for energy dissipation and/or controlled behaviour after peak load can therefore exclude LWAC as the preferred material. The main objective of this

research was to increase our understanding of the ultimate response of LWAC members in compression and bending [14].The background was that the common explanations for the differences between LWAC and NWC were not entirely satisfactory. Very often the experimental results seemed to be in conflict with the current way of thinking [15]. The hypothesis underlying this study was that the three key material characteristics that generally determine the ultimate response of concrete structures are: the large effect small secondary stresses have on the compressive strength; the abrupt increase of the transverse expansion at a stage close to, but not beyond, the peak stress level; and the rapid unloading of the material beyond the peak stress level. It follows from these features that the strength, and especially the ductility, of structural concrete members depend on local triaxial stress conditions that inevitably develop in the compressive zone prior to failure, rather than on stress-redistributions due to post-peak material characteristics, as is commonly believed. This hypothesis has previously been used with success to explain and predict the behaviour of NWC members in the ultimate limit state [16, 17]. This research aimed to find out whether it can be used to explain the experimental results that seem to be in conflict with the current theoretical understanding of the ultimate response of LWAC members. So the main goal of this work was to investigate the explanatory power of the alternative hypothesis when applied to LWAC. In this respect, a large variety of experimental data reported in the literature were examined. Existing triaxial strength data were used as the basis for the development of a novel failure criterion taking into account the density of the concrete. Finally, a three-dimensional nonlinear FE model with the proposed failure criterion was developed for the verification of the hypothesis.

2 Fundamental behaviour of concrete at material level

2.1 **Underlying reasons for the differences between LWAC and NWC**

Aggregates make up the highest volume fraction in a concrete. The primary reason for mixing aggregate with cement paste is to reduce the cost of the material, since aggregates are cheaper than cement. Moreover, aggregates reduce shrinkage and creep, give better volume stability in the concrete, and enhance its durability. In NWC, the strength of the aggregate is rarely a problem, and the properties of the aggregates therefore do not determine the performance of the concrete. The lower overall density of LWAC is achieved

by replacing the conventional gravel aggregates with lighter and, therefore, softer and weaker types. So the aggregates in LWAC are more prone to affect the performance of the concrete, and will in many cases become the decisive factor. The porous nature of the lightweight particles means that the cement paste tends to penetrate inside the aggregates, resulting in little or no transition zone between the component phases. So what primarily sets LWAC apart from NWC is: a lighter, softer and weaker aggregate compared to the mortar, combined with an often higher bond strength between these two components.

Concrete can be separated into two classes determined by the properties of the two components, aggregate and mortar [18]. In the first class of concretes, including ordinary NWC and some lightweight concretes, the concrete composite can be considered as a two-phase material in which stiffer and stronger particles are embedded in a softer and weaker matrix. The short-term strength is a function of the strength of the mortar only, which predominantly depends on the water-cement ratio of the mix and the strength of the cement. In the second class of concretes, where softer and weaker particles are embedded in a stronger and stiffer matrix, the influence of the aggregates on the strength must be taken into account. The effect of the aggregates on the overall compressive concrete strength can be evaluated by comparing the relationship between the strength of the mortar and the strength of the concrete made with this mortar, as illustrated in Figure 1.

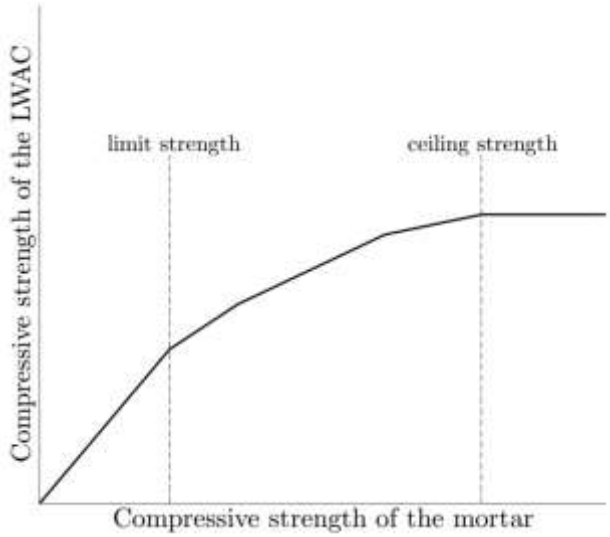

Fig. 1. Relationship between the strength of the mortar and of LWAC made with the same mortar.

Up to a certain limit, the compressive strength of the concrete will be governed by the compressive strength of the mortar. The limit marks the shift from what can be defined as a class one to a class two concrete. Below the limit strength, a lightweight concrete behaves in the same way as an ordinary concrete. However, above the limit strength, the stress distribution within the concrete will be different due to the inversion of the stiffness characteristics of the component phases, with the mortar now sustaining a greater part of the load as illustrated in Figure 2. The final failure of the class two concretes will be initiated by the splitting of the aggregates, as a result of their lower strength and the effect of the tensile stress concentrations now being located immediately above and below the aggregate particles. When the tensile stress concentrations exceed the strain-energy capacity of the material in these regions, microcracks propagate into the mortar. More external load can be applied to the concrete only if the stress that can no longer be transferred across the crack can be redistributed. If the bond between the aggregate and the cement-mortar is strong enough, the diverted stress can be taken up by the aggregate. This is why the propagation of microcracks into the mortar increases the stress to be taken up by the aggregate, which eventually fails by splitting when its tensile strength is exceeded. Concrete made of a certain type of aggregate can be made progressively stronger by increasing the strength of the mortar. However, increasing the strength of the mortar can only compensate for the weakness of the aggregate up to a certain limit depending on the tensile strength of the aggregate. This strength value is referred to as the ceiling strength of the concrete.

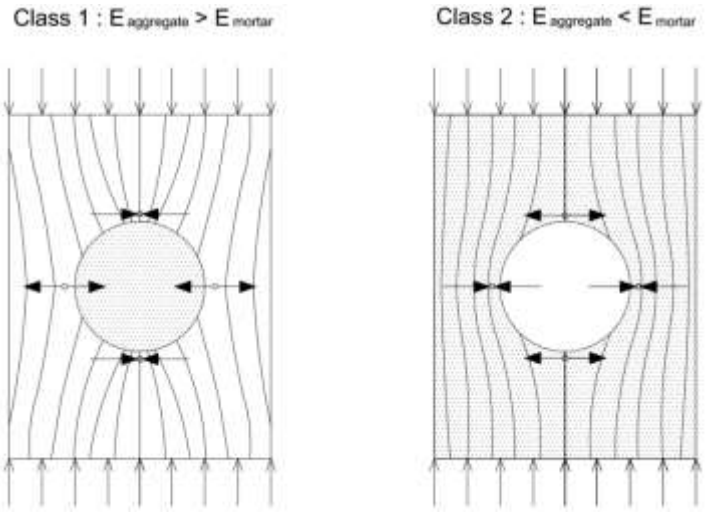

Fig. 2. Internal stress transfer in concrete under a compressive load [19].

An important implication of the above reasoning is that there is no clear-cut division between NWC and LWAC, and the best indication of the anticipated concrete behaviour seems to be given by the relationship between the relative strength and stiffness characteristics of the component phases of the particular concrete mix.

2.2 **Concrete in uniaxial compression**

It is widely believed that knowledge of the complete stress-strain curve under uniaxial compression, i.e. including the descending branch, is essential for structural analysis [20]. The descending branch is often termed the softening branch and describes the specimen's gradual loss of load-carrying capacity after the peak load for increasing deformation. When the softening branch is steep, the specimen is said to behave in a brittle manner, whereas when the softening branch is nearly horizontal, the specimen is said to exhibit a nearly ductile behaviour. Figure 3 shows examples of stress-strain relationships for use in non-linear structural analysis according to Eurocode 2 (EC2) [21]. NWC is assumed to exhibit rather ductile behaviour, while LWAC is assumed to suffer a completely brittle failure regardless of its composition. This implies a sharp distinction between NWC and LWAC. This is unfortunate because it might prevent the use of quite straightforward lightweight mixes, e.g. using a strong lightweight aggregate to compose a concrete of relatively modest strength. For such mixes, it is hardly at all justifiable to treat LWAC as a different material. The highly linear stress-strain behaviour up to failure for LWAC is a result of little or no microcracking.

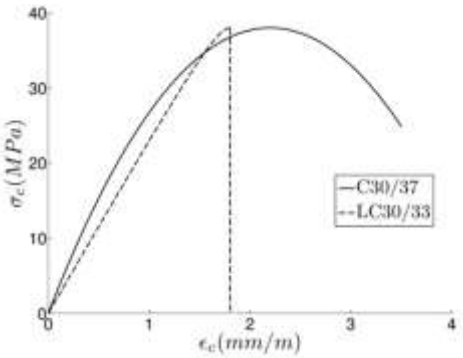

Fig. 3. Stress-strain relationship for non-linear structural analysis for NWC and LWAC according to Eurocode 2.

The complete stress-strain curve under uniaxial compression can be established from deformation-controlled tests when an energy-absorbing 'stiff' testing machine is used. Normally, tests are performed on cylindrical

specimens that are twice as long as their diameter and loaded through rigid steel plates. At a stage close to but not beyond the peak stress level, visible cracks form in the direction of the applied load. These cracks will be limited to the central section of the specimen due to the confining stress in the end sections. The void formation caused by the cracks will therefore lead to a highly incompatible lateral deformation profile over the height of the specimen. As a response, internal forces develop which act so as to restrain the expansion of the central zone and, in contrast, increase the expansion of the end zones. The expanding forces eventually overcome the confining stress in the end zones, and when the strength criterion of the concrete in compression/tension is met, the cracks propagate into the specimen ends and trigger the ultimate collapse. This means that only the ascending portion of the stress-strain curve up to the minimum-volume level describes the deformational behaviour of an element of concrete under a well-defined state of stress. Tests where attempts have been made to reduce the friction between the loading plates and the specimen, demonstrate that the steepness of the descending branch increases as a function of the efficiency of the friction-reducing measures [22]. This effect can be clearly seen in Figure 4.

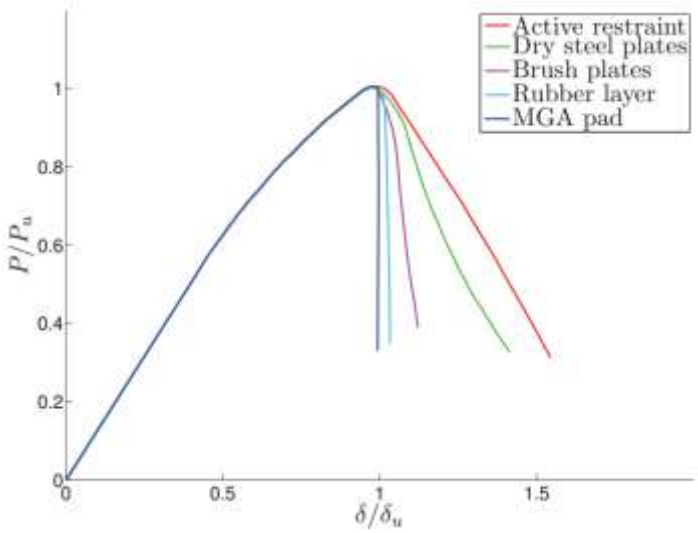

Fig. 4. Load-deformation relationships established from cylindrical specimens, for various amounts of boundary restraint [23].

A great deal of the scepticism about the use of LWAC for structural applications is concerned with the steepness of the descending portion of the stress-strain curve in compression. However, according to the foregoing, the post-peak behaviour of any concrete should be described with a 90 degree slope of the descending portion of the stress-strain curve, irrespective of its composition. The various strain-softening

branches that can be measured in the laboratory can be explained by the various sizes of the triaxially confined end zones. The depth of these zones will depend on the size, distribution and volume percentage of aggregate, and the stiffness of the aggregate relative to that of the mortar. For a fine-grained mix where the stiffness characteristics of the aggregate and the mortar are close together, the distance from the loaded boundaries required to ensure a nearly-uniform state of uniaxial compression will be smaller than that of a coarse-grained mix with incompatible stiffness characteristics of the component phases . For mixes where the stiffness characteristics of the component phases are brought closer together, either by decreasing the stiffness of the aggregate (LWAC) or by increasing the stiffness of the mortar, this means that the triaxially confined end zones will become smaller. Since it is the restraint from the end zones that gives rise to the post-peak behaviour, this will result in a downward shift of the descending portion of the stress-strain curves for these concretes.

2.3 **Concrete under multiaxial states of stress**

It is well known that confinement increases the ductility of concrete as well as enhancing its strength. Moreover, an active confinement from external stresses is more effective than a passive confinement mobilised by an opposing transverse deformation from the Poisson effect. Numerous researchers have investigated the confinement effect in concrete, both experimentally and theoretically [24-26]. This paper emphasises the effect of local triaxial stresses that inevitably develop in the compressive zone just prior to failure in the strength and especially the ductility of structural concrete members. This requires a proper description of concrete under multiaxial states of stress combined with a proper description of the increase of the transverse expansion of concrete close to the peak stress level [9].

Multiaxial material data can be obtained either by loading cubes between dry steel plates, lubricated steel plates, brush plates, or fluid cushions, or by adding a fluid pressure test to the standard uniaxial cylinder test. An international test programme found that the lateral boundary constraint was the main influence on the specimen behaviour [27]. This means that loading techniques that do not aim to eliminate shear stresses on the specimen surface should be disregarded altogether, i.e. dry rigid steel plates should not be used. The triaxial cylinder test is probably the best to use, because the deformational response can readily be obtained from strain gauges mounted onto the central zone subjected to a well-defined triaxial state of stress up to the

minimum-volume level. The only drawback is that two of the principal stresses must at all times be equal, but this will rarely be an issue. A uniform strain in the contact zone of the loading device and the specimen is preferable, because what is sought is the overall response of specimens which are sufficiently large to represent the average properties of what is really a heterogeneous mix.

A typical failure surface in the principal stress space is shown in Figure 5. In the axi-symmetric stress plane, the strengths are limited by an upper compression meridian and a lower tension meridian. It is interesting to note that complete stress-strain curves can be measured in the triaxial ‘compression’ tests, but not in the triaxial ‘extension’ tests [28]. This is believed to be a result of the different orientation of the crack propagation process in the two cases. Cracks always propagate in the direction of the maximum principal compressive stress and will therefore be orientated in the axial and transverse directions in these two cases respectively.

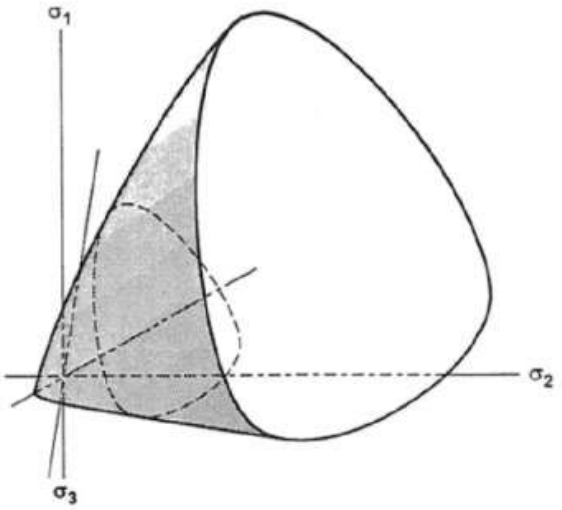

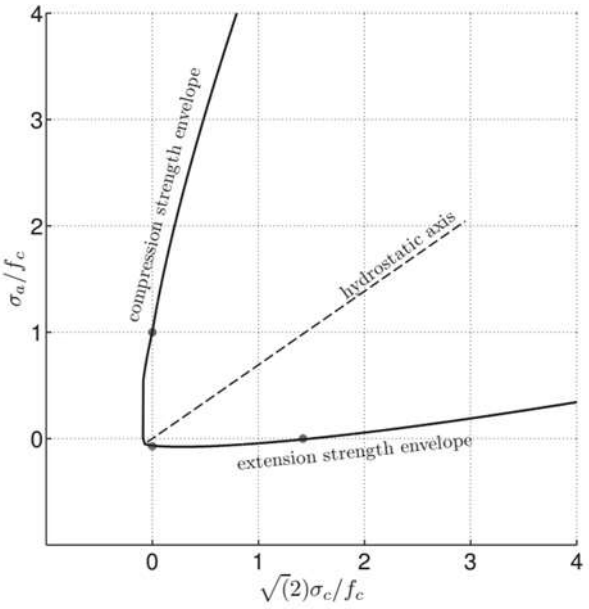

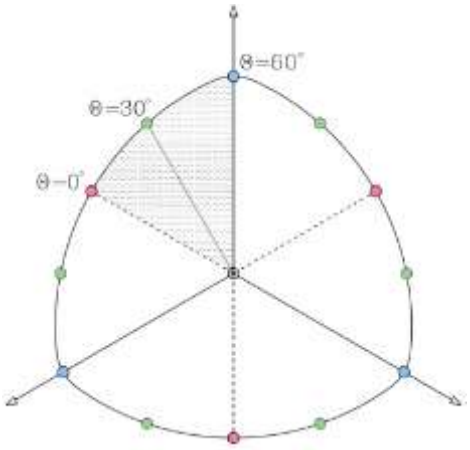

Fig. 5. Typical failure surfaces in the principal stress, axi-symmetric and deviatoric plane.

The response under multiaxial states of stress can be divided into three parts: the change in volume due to hydrostatic loading; the change of shape due to deviatoric loading; the change in volume due to deviatoric loading. In constitutive modelling of multiaxial states of stress, therefore, it is convenient to use an octahedral formulation. The octahedral coordinates are defined by a vector on the hydrostatic axis, ξ, a vector in the deviatoric plane, ρ, and the rotational variable on the deviatoric plane, θ, defined by:

$$\xi = \frac{1}{\sqrt{3}}\mathrm{I}_1, \quad \rho = \sqrt{2J_2}, \quad \cos 3\theta = \frac{3\sqrt{3}J_3}{2J_2^{3/2}} \tag{1}$$

where I_1 is the first invariant of the stress tensor and J_2 and J_3 are the second and third invariants of the deviatoric part of the stress tensor. Moreover, as an alternative to represent the failure criterion in the principal stress space, the octahedral stress space is often used as a coordinate system. The hydrostatic and deviatoric components of the stress tensor are then expressed in terms of the normal octahedral stress σ_0 and the shear octahedral stress τ_0, which are defined as:

$$\sigma_0 = \frac{\xi}{\sqrt{3}}, \quad \tau_0 = \frac{\rho}{\sqrt{3}} \tag{2}$$

Since concrete can be considered to be isotropic before the failure surface appears, i.e. sixfold symmetry of the failure surface can be assumed, the strength data from these load paths is sufficient to fully define the deviatoric plane. If such strength data can be determined for an adequate number of hydrostatic stress levels, mathematical expressions for the entire failure surface can be derived. The meridians represent the intersection curves between the failure surface and a plane containing the hydrostatic axis with θ being constant. The state of stress on the meridians has two equal principal stresses. On the compressive meridian (θ=60º), they are greater than the third, on the tensile meridian (θ=0º) they are smaller.

The advantage of adopting an octahedral formulation of the material data is that the same relationships can be used to express uniaxial, biaxial and triaxial concrete behaviour, i.e. the material model can be used to describe the behaviour of concrete under generalised states of stress [29]. The strength and constitutive relationships are obtained directly by fitting curves to material data from multiaxial tests. Obviously, this requires a lot of testing at the material level. For concrete, however, this seems to be the best option because,

as stated in the CEB-FIP state-of-the-art report on finite-element modelling of reinforced concrete structures [6], 'concrete is a complex and stubborn material that sometimes refuses to act according to accepted rules of mechanics'. So it can be argued that empirically fitted curves are preferable to the classical continuum mechanics formulations, because the latter seem to be too much of a straightjacket for the mathematical descriptions and do not seem to provide a sound theoretical foundation for the material behaviour.

3 Alternative explanation for the failure of RC members

3.1 Characteristic types of ultimate behaviour

The most common way of investigating the behaviour of reinforced concrete (RC) members in bending is by loading simply supported beams symmetrically about the mid-section using two point-loads (four-point bending). This test method combines two test conditions: constant moment in the central section, and combined shear and flexure in the two end sections. Whether the moment capacity attained, M_c, reaches the full flexural capacity, M_f, of a given beam, depends on the amount of flexural reinforcement and on the ratio between the length of the shear span, a, and the effective depth of the beam d. The behaviour of beams without shear reinforcement can be divided into four distinct types depending on the a/d ratio, as illustrated in Figure 6.

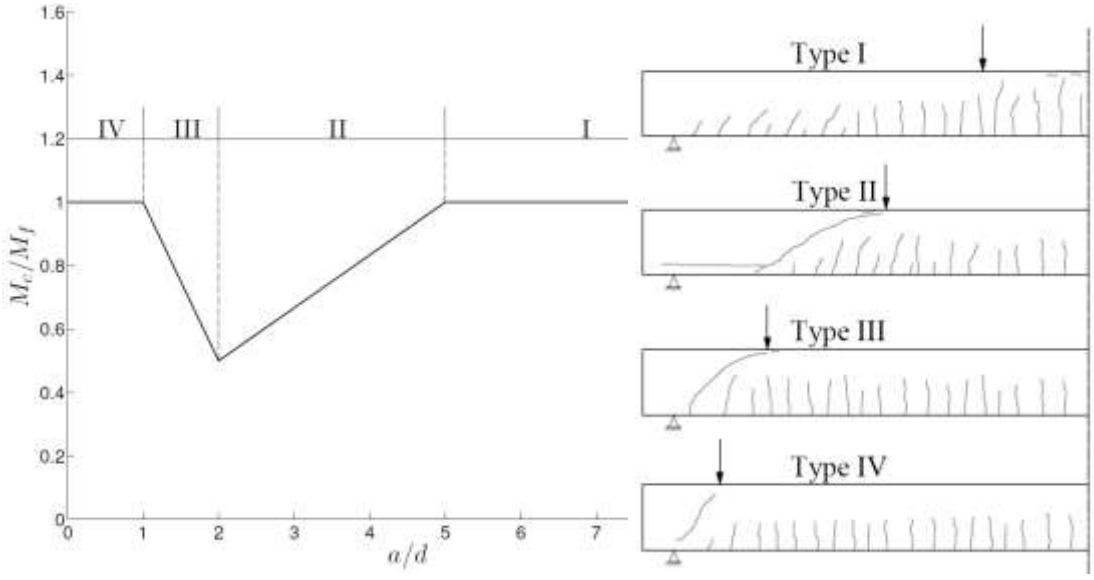

Fig. 6. Characteristic types of ultimate behaviour for beams without transverse reinforcement [30].

The non-flexural types of failure, apart from those associated with loss of anchorage or bearing failure in regions of point loads (which are usually prevented by proper detailing), are collectively referred to in the literature as shear failures (also in this paper). The reason for this is that they generally occur only if there is a shear force present, and they are normally characterised by diagonal cracks in the shear spans. Nonetheless, this term is somewhat misleading, since it gives the false impression that failure occurs when the shear stress exceeds the shear capacity of the concrete at a critical cross-section. That this is not the case was pointed out by P.M. Ferguson as long ago as 1952 [31], when he conclusively demonstrated that the shear stress at failure very much depends on the *a/d* ratio.

The response of the beams in Figure 6 beams forms a comb-like structure in which the uncracked concrete in compression forms the backbone of the comb. The hypothesis of this paper is that the four types of ultimate behaviour can be explained by the stress conditions in the compressive backbone of the beams, denoted by the compressive force path (CFP) [32], see Figure 7. Failure of the CFP is most likely due to development of secondary tensile stresses. Such stresses may develop for a variety of reasons, the main ones being related to changes in the direction of the CFP, the varying intensity of the compressive stress field along the CFP, bond failure, or stress concentrations at the tips of inclined cracks.

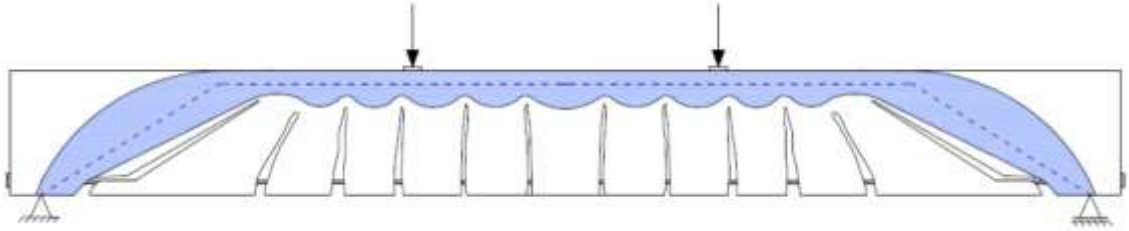

Fig. 7. The compressive force path.

Type I failures typically have a flexural crack in the middle portion of the beam that penetrates deep into the compressive zone. This intensifies the compressive stress and increases the transverse expansion in a localised region of the CFP, which for equilibrium and compatibility reasons results in longitudinal splitting of the adjacent concrete when the strength of the concrete in a compression-tension-tension zone is exceeded. This type of failure is typical for *a/d* ratios greater than 5 and will be of the desired flexural type.

Type II failures are characterised by the flexural crack closest to the support turning into an inclined crack which immediately propagates nearly horizontally into the compressive zone towards the point load. The crack might also propagate along the tensile reinforcement towards the support, destroying the bond. This might lead to an anchorage failure. These effects result in a sharpening in the kink of the CFP in the region of the tip of the inclined crack, which for equilibrium reasons produces a tensile stress resultant. This tends to pull the compressive zone apart between the tip of the inclined crack and the top face of the beam. Another cause of the near horizontal splitting of the compressive zone might be the large tensile stresses that act at the tip of the inclined crack. Moreover, a local loss of bond between the flexural reinforcement and the concrete can also induce tensile stresses in the CFP, because the new equilibrium condition then requires the nearby flexural crack to lengthen, which boosts the compressive stress in a localised region of the CFP, which as a response induces tensile stresses in the adjacent regions. These types of failure are typical for *a/d* ratios between 2 and 5 and will not be of the desired flexural type.

Type III failures have a deep inclined crack that initiates at the bottom face near the support and propagates towards the point load. Unlike the inclined crack characterising Type II behaviour, this does not lead to immediate failure. Instead, further load can be applied until the concrete adjacent to the tip of the inclined crack splits in the longitudinal direction as a response to the large transverse expansion of the highly stressed region above the crack tip. This kind of failure is typical for *a/d* ratios between 1 and 2 and will be of the undesired non-flexural type, because the inclined crack penetrates deeper into the compressive zone than the flexural crack causing Type I failure. The full flexural capacity of the beam can be obtained by locating transverse reinforcement in the region of the shear span.

Type IV failures are characterised by an inclined crack that initiates within the beam web almost half way between the load and support and at a load level well below the load-carrying capacity. This crack propagates simultaneously towards the load point and the support with increasing load and eventually causes failure due to a sudden extension of the crack in both directions. This kind of failure is typical for *a/d* ratios below 1 and is brittle, although the full load-carrying capacity is normally achieved. For larger beam sizes, failure can instead be caused by inclined cracks penetrating deep into the compressive zone in the middle portion of the beam. The failure mechanism here is the same as for the Type III behaviour, but the failure

will be flexural because the cracks do not propagate any deeper than the flexural cracks characterising Type I behaviour.

The above description of various types of failure is based on tests of NWC members. The question remains whether LWAC members act in a similar manner. This question is examined in the following for failure Types I, II and III, by carefully investigating experimental data from the literature.

3.2 **Flexural failure**

The behaviour of slender RC beams subjected to gradually increasing load is thought to be well known, but an alternative explanation based on the properties of concrete under multiaxial stress may better describe the behaviour observed. Figure 8 shows a typical cracking pattern for a flexure failure. At a load level close to failure, there is a dramatic increase in the compressive stress in localised regions above the bending cracks, partly due to the increase in load, but mainly as a result of the reduced area of the compressive zone. The concrete in these regions will therefore expand far more than the concrete in the adjacent regions. This is a result of the distinct increase in the Poisson's ratio of the concrete as failure is approached. Strain compatibility and static equilibrium then require confining stresses in the highly stressed regions and tensile stresses in the adjacent regions which do the restraining. This must inevitably influence the response of the beam, since the compressive load-carrying capacity of concrete is extremely sensitive to even small secondary stresses. Compressive stresses increase the load-carrying capacity considerably, while tensile stresses have a dramatic and opposite effect. This means that the development of secondary stresses allows for bending stresses far in excess of the uniaxial strength in regions above deep cracks at the expense of the strength of the concrete in adjacent regions.

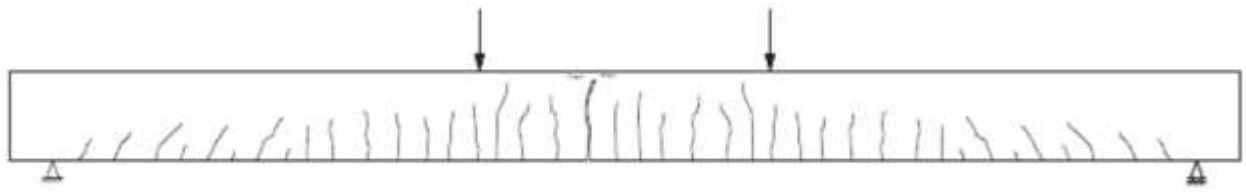

Fig. 8. Typical flexural failure of an RC beam.

The large strains that can be measured on the compressive face of a flexural RC member seem therefore to be a result of the development of compressive stresses in excess of the uniaxial strength rather than stress redistributions due to post-peak stress-strain characteristics, as is commonly believed. The fact that the compressive zone shows no visible sign of distress until the moment of structural collapse strongly supports this claim. If the stress conditions in the compressive zone really were uniaxial during the entire loading range, cracks would be expected to occur in the beam's top face when the strain in the axial direction exceeds 0.002, which is the typical strain level at cracking in uniaxial cylinder tests. Instead, the formation of longitudinal cracks occurs at the moment of structural collapse in the zones adjacent to the deepest flexural crack, as illustrated in Figure 8, which is highly suggestive of a tensile failure in these regions. Concrete crushing is then merely a post-failure phenomenon caused by the loss of restraint previously provided by the adjacent concrete.

In view of the above, the ductility of bending RC members should depend on the local triaxial stress conditions that develop in the compressive zone just prior to failure. A high degree of stress triaxiality in the compressive zone will result in large local compressive strains that form local 'hinges' that can account for the overall ductility of the member. The often limited ductility of LWAC members seems therefore to be due to a low degree of stress triaxiality in the member due to a smaller transverse expansion of the concrete prior to failure. For LWAC mixes close to or at the ceiling strength, it can also be supposed that concrete crushing of the highly-stressed region above the deepest crack precedes tensile splitting of the adjacent regions, as a result of the smaller triaxial strength gain for these types of mixes.

To support the above argumentation, strain distributions from an experimental programme found in the literature [33] were investigated. The programme included simply supported NWC and LWAC beams, both under-reinforced and over-reinforced, and subjected to four-point loading with an a/d ratio of 5. Figure 9 shows the longitudinal compressive strains on the top surface of the constant moment region for some of the beams tested. This shows that the localisation of strains took place in regions above deep flexural cracks just prior to failure at about 90% of the load-carrying capacity of the beam. This is fully in agreement with the failure mechanism put forward above, where local triaxial stress conditions and therefore large local strains

are expected to develop above deep cracks. The localisation of strains in the compressive zone of bending RC members prior to failure is generally acknowledged by the research community, but it is normally associated with the post-peak stress-strain characteristics of the material. Figure 9 also shows that the strain concentrations in the compressive zone were generally less pronounced for the over-reinforced beams, especially for the LWAC beam. This is probably a result of the limited degree of stress triaxiality in these members due to a low bending moment gradient and a small transversal expansion of the concrete prior to failure.

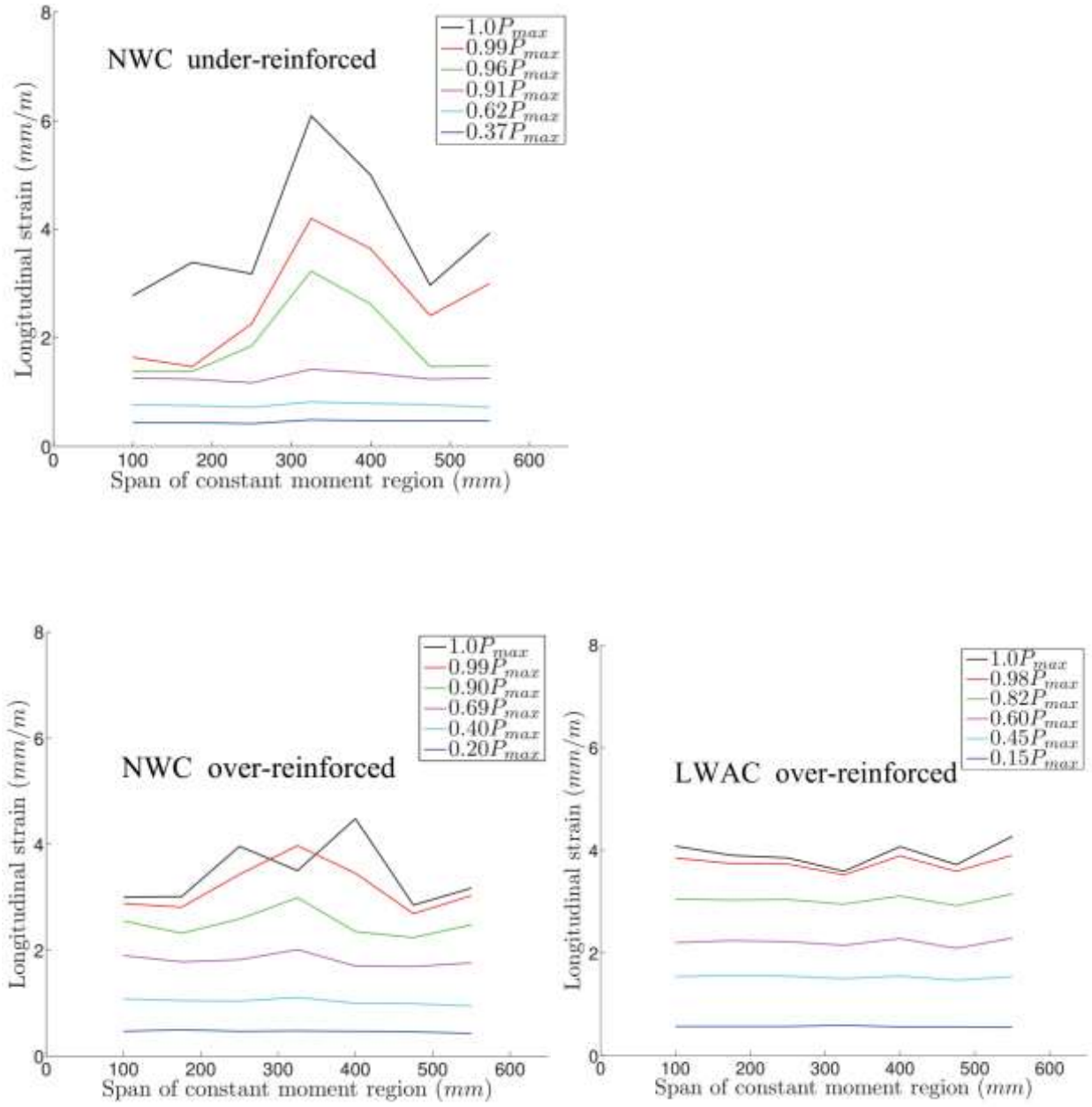

Fig. 9. Longitudinal compressive strain profile [33].

This means that no experimental uniaxial stress-strain curve can realistically describe the response of the concrete in the compressive zone as failure is approached, for the simple reason that the stress conditions in the compressive zone will then no longer be uniaxial. The effort put into measuring the post-peak branches of the stress-strain curves may therefore very well be wasted, since these parts of the curves can at best only provide indirect information about the expected material response. Nonetheless, empirically-fitted uniaxial models seem to be the only practical method for carrying out simple hand-calculations, and these models are able to predict the behaviour of standard members very well. However, FE analyses should be aimed at achieving a material description that captures all the essential features governing the structural response, which, in the case of concrete, means taking the triaxial effects adequately into account.

The test programme also measured the transversal strain on the top face of the beams and in cylinder tests. Figure 10 presents typical relationships found between longitudinal and transversal strains. It shows that, for a given longitudinal compressive strain, the corresponding transversal tensile strain is higher for the over-reinforced beams than for the under-reinforced ones. This means that the restraint of the highly stressed regions is less in the former case. This seems to reflect the fact that the curvature of the over-reinforced beams is smaller – an effect that has been found to significantly decrease the degree of stress triaxiality in the compressive zone.

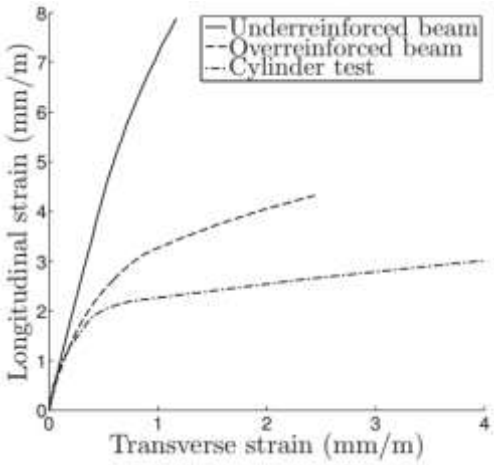

Fig. 10. Relationship between longitudinal and transversal strain [33].

Strain data from the beam tests revealed very high curvatures in the 'plastic' regions above deep flexural cracks prior to failure. The large curvatures in these regions seemed to result in a relatively large vertical component in the longitudinal compressive force, whose effect on the concrete behaviour could not be neglected. The low degree of stress triaxiality in the compressive zone of the over-reinforced beams may therefore be a result of a low beam-bending curvature. Moreover, the compressive zone will be larger in these beams. This means that the variation in the transverse expansion along the beam axis will be less pronounced, which also seems to result in a lower restraint of the highly-stressed regions and therefore a lower degree of stress triaxiality in the compressive zone.

Figure 10 also compares the beam strains with typical axial strain-lateral strain relationship obtained from standard uniaxial cylinder tests. The two distinct portions of the cylinder test curve correspond to the ascending and the descending branches of the axial stress-axial strain and axial stress-lateral strain curves respectively. This comparison demonstrates quite conclusively that while the ascending portion of the stress-strain curve describes the deformational behaviour of an element of concrete in the compressive zone of a bending RC member fairly well, the descending portion does not. The reason for this must be the triaxial stress conditions that develop in the compressive zone prior to failure.

3.3 **Non-flexural failure**

There is still no generally accepted rational theory for predicting the strengths of RC members that suffer non-flexural failure. It is commonly believed that the shear capacity of RC members without stirrups is made up of contributions from the uncracked concrete in the compressive zone, aggregate interlock, and the dowel action of the flexural reinforcement crossing the cracks. According to tests by Fenwick and Paulay, the size of these contributions can be taken as approximately 20% for the uncracked concrete in the compressive zone, 20% for the dowel action, and 60% for the aggregate interlock [34]. However, there are several arguments indicating a negligible contribution from the two latter mechanisms. These arguments can be summarised as follows:

1. The conviction that aggregate interlock makes the most significant contribution to the 'shear' capacity is, to a large degree, based on the tests by Fenwick and Paulay [34]. In these tests, pre-

formed cracks were cast into RC beams below the neutral axis by pre-inserting sheet metal strips in the forms. This was done to eliminate the transfer of forces across the cracks. Since this reduced the load-carrying capacities of the beams by about 30% compared to similar beams without pre-formed cracks, it was concluded that the contribution from aggregate interlock had to be responsible. However, numerical simulations, where the effect of aggregate interlock has been neglected, have indicated that the mere introduction of pre-formed cracks might cause the load-carrying capacity to decrease by a similar amount. This puts the conclusion from the work of Fenwick and Paulay and other similar experiments into question.

2. The contributions from aggregate interlock and dowel action can only be effected by shear deformation of the crack surfaces. This contradicts the fundamental crack mechanism of concrete. Cracks propagate in the direction of the maximum principal compressive stress and open up in the orthogonal direction. This means that no significant shear deformations between the crack surfaces are likely before failure.
3. The contribution from aggregate interlock is only relevant after the concrete in the compressive zone has cracked, because the stiff compressive zone before cracking is likely to sustain the entire shear force. The contribution from aggregate interlock must therefore be negligible as long as the compressive zone remains uncracked. This means that the contributions of the uncracked concrete and the aggregate interlock cannot be added together.
4. According to Reinhardt and Walraven, aggregate interlock is ineffective after the crack width exceeds about 1mm [35]. However, 'shear' tests of RC beams without transverse reinforcement have shown that the load-carrying capacity can increase significantly even after crack widths greatly exceed 1mm [36].
5. The cracked surfaces are smoother in LWAC members than in NWC members. This means that if aggregate interlock really was the main contributor to the 'shear' resistance, we would expect that the load-carrying capacity of lightweight 'shear' beams would be poor. However, the load-carrying capacity of such members is often as good, nearly as good, or even better than that of their normal-weight counterparts [37].
6. Reinforced concrete T-beams with a web width significantly smaller than that generally considered to provide adequate shear resistance can still achieve full flexural capacity [36].

7. The contribution from dowel action must be a function of the stiffness and therefore the diameter of the steel bars. However, 'shear' tests of RC beams where the diameters of the steel bars have been varied, while the total cross-sectional area and the centre of gravity of the bars has been kept constant, have not shown any reduction in load-carrying capacity with decreasing bar diameter [38].

From the above reasoning, it can be concluded that the uncracked concrete in the compressive zone is the main contributor to the 'shear' capacity of RC members, with the mechanisms of aggregate interlock and dowel action being small enough to be neglected. This explains why the shear stresses increase considerably in cross-sections above deep cracks when cracks penetrate deep into the compressive zone. However, the compressive zone does not suffer any visible signs of distress until the moment of structural collapse, even when the cracks penetrate very deeply into the compressive zone. This can be explained by the triaxial stresses that inevitably develop above deep cracks. The vertical component of the triaxial stress state will counteract the tensile stresses in the compressive zone. This allows for shear stresses far above those normally expected to be sustained by the compressive zone.

From the description of failure types in Section 3.1, the load-carrying capacity of LWAC and NWC members can be expected to be rather similar in most cases. This is because RC members are very much prone to fail by violation of the strength criterion of the concrete in the compressive/tensile regions of the compressive force path, for which the differences are assumed not to be substantial. However, the load-carrying capacity of heavily reinforced Type III beams made of low density concrete can be expected to be low. This is due to the degree of stress triaxiality, which tends to decrease with decreasing density with a corresponding decrease in triaxial compressive strength, so that regions above deep cracks might fail prematurely due to concrete crushing. This will be most critical for the Type III beams, because the inclined cracks then tend to penetrate very deeply into the compressive zone at a load level well below that corresponding to the yielding of the flexural reinforcement.

Results from tests on RC members made of LWAC that were carried out at SINTEF [39, 40] were used to evaluate the above hypothesis. The results were also compared to results from similar tests of NWC beams

conducted at the University of Toronto [41]. The Toronto tests were studied over a wide range of *a/d* ratios, and the 'shear valleys' in Figure 6 were found to be almost independent of the strength of the concrete.

Figures 11 and 12 compare the 'shear valleys' from the Toronto tests with 1.88 and 2.80% steel with the relative strengths of the SINTEF beams with 1.8 and 3.0% of steel respectively. These steel percentages are similar enough to provide an adequate comparison, and this seems to show that the working hypothesis is correct. For the Type II failures, where the strength of the concrete in compression/tension or the steel-concrete bond strength is considered to be important, no alarming differences can be seen. In fact in many cases, the LWAC beams perform better than their normal-weight counterparts. Perhaps this was due to a better bond between the concrete and the reinforcement, since this tends to influence the stress conditions in compressive zone in the region above. However, in the case of the Type III failures, the relative strength of the LWAC beams, especially the heavily reinforced ones with the lowest density, falls below that of their normal-weight counterparts. This means that the flexural reinforcement is far from having reached its yield strain when the load-carrying capacity of the beams is reached. This means that it would be very difficult to achieve a ductile beam failure in these cases. It would necessarily require a large amount of additional transverse steel, whose weight would necessarily cancel out a substantial part of the weight saving from the reduced density of the concrete.

As a last remark, it should be noted that the above reasoning does not shake the validity of current design rules, since these are concerned with the inclined cracking load and not the ultimate load-carrying capacity of the members. But it might have some consequence for the ductility of RC members under possible overload conditions, such as earthquakes.

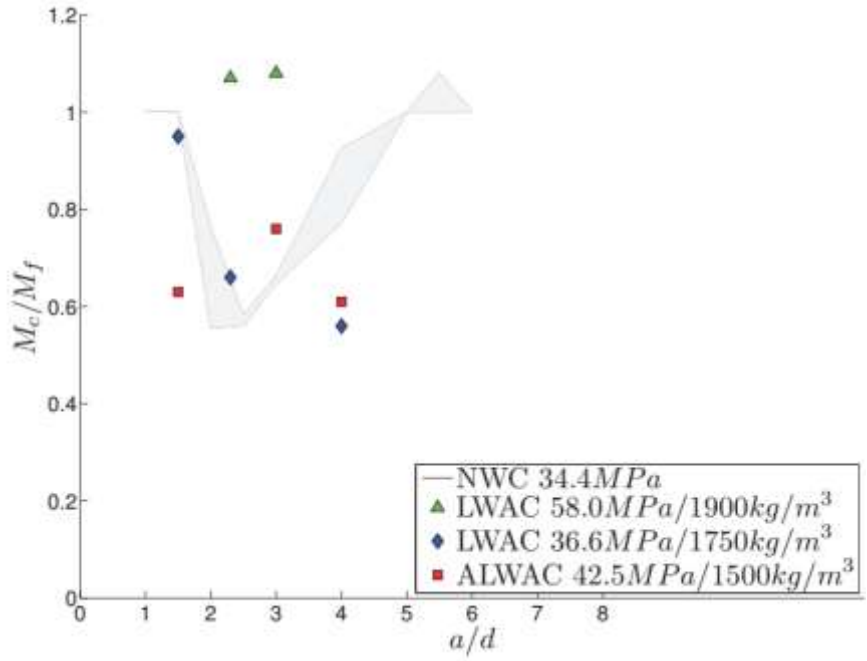

Fig. 11. Relative beam strengths for various *a/d* ratios for 1.8% longitudinal reinforcement compared to Kani's valley [41].

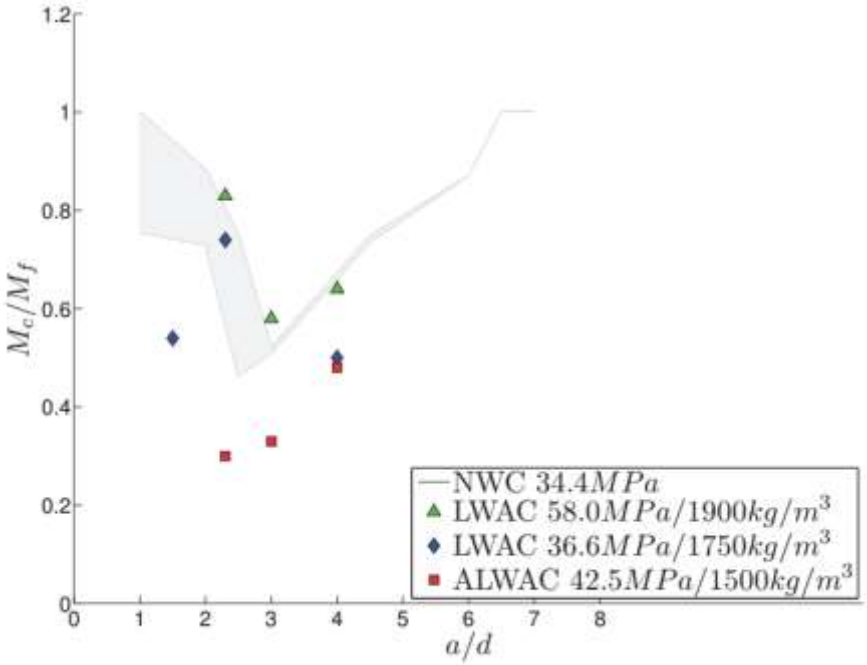

Fig. 12. Relative beam strengths for various *a/d* ratios for 3.0% longitudinal reinforcement compared to Kani's valley [41].

4 Material model for NLFEA

4.1 Constitutive relation

As part of the verification and exploratory process to get a better understanding of the behaviour of LWAC, nonlinear finite element analyses (NLFEA) were carried out. The working hypothesis in this research focused on the importance on the triaxial stress conditions in compressive zones and the rapid unloading of the material beyond the peak stress level. The present work was therefore based on a brittle fully triaxial material model for concrete in order to describe the non-linear deformational response to an increasing state of stress. This model has previously been implemented in a smeared, non-orthogonal, fixed cracking framework by several authors [17, 42, 43]. The material model was derived by curve-fitting of deformational data from axi-symmetric tests. It is based on the following assumptions:

- Under hydrostatic stress (σ_o), concrete only develops hydrostatic strains (ε_{oh}).
- Under deviatoric stress (τ_o), concrete develops both deviatoric (γ_o) and hydrostatic strains (ε_{od}).
- The deviatoric stress-strain relationships ($\tau_o - \gamma_o$) are independent of the hydrostatic stress applied.
- The influence of the rotational variable θ is negligible.

According to these assumptions, the stress-strain relations can be written in the following form:

$$\varepsilon_0 = \varepsilon_{oh} + \varepsilon_{od} = \frac{\sigma_0 + \sigma_{id}}{3K_s} \tag{3}$$

$$\gamma_0 = \frac{\tau_0}{2G_s} \tag{4}$$

where $\sigma_{id}(\sigma_o, \tau_o, f_c)$ is an equivalent hydrostatic stress that accounts for the coupling between deviatoric stress and hydrostatic strain, and $K_s(\sigma_o, f_c)$ and $G_s(\tau_o, f_c)$ are the secant bulk and shear moduli when this coupling is ignored. Expressions for K_s, G_s, and σ_{id} were derived by curve-fitting of uniaxial, biaxial and triaxial data, and can be found in [44]. The material model defined by Equations 3 and 4 deviates from isotropic nonlinear elasticity only by the hydrostatic correction term. The constitutive relation describing the state of strain corresponding to any state of stress is therefore equivalent to the following relationship in global directions:

$$\varepsilon_{ij} = \frac{\sigma_{ij} + \sigma_{id}\delta_{ij}}{2G_s} - \frac{3\upsilon_s(\sigma_0 + \sigma_{id}\delta_{ij})}{E_s} \tag{5}$$

where δ_{ij} is the Kronecker delta, and $E_s(\sigma_o, \tau_o, f_c)$ and $\nu_s(\sigma_o, \tau_o, f_c)$ are the Young's modulus and Poisson's ratio from the standard elastic expressions.

4.2 **Density-dependent octahedral failure criterion**

In its original form, the failure criterion in the constitutive relation described in the previous section was valid for NWC and given for the compressive meridian (θ=60º) and the extension meridian (θ=0º) as:

$$\frac{\tau_{oc}}{f_c} = k_1\left(\frac{\sigma_0}{f_c} + 0.05\right)^{k_2} \quad \text{where } k_1 = 0.944 \text{ and } k_2 = 0.724 \tag{6}$$

$$\frac{\tau_{oe}}{f_c} = k_3\left(\frac{\sigma_0}{f_c} + 0.05\right)^{k_4} \quad \text{where } k_3 = 0.633 \text{ and } k_4 = 0.857 \tag{7}$$

Furthermore, the meridians for any θ intermediate between 0º and 60º can be described by the interpolating function according to William and Warnke [45]. So, assuming sixfold symmetry, i.e. isotropic behaviour, once the variations of τ_{oc} and τ_{oe}, with σ_o have been determined, the entire failure surface is defined.

The validity of the criterion was extended by proposing a density-dependent failure criterion for LWAC. A full description and derivation of this criterion can be found in [14, 46]. The derivation was based on strength data from a test programme for concretes of varying densities [47]. The following modification is proposed for the *k*-factors in Equations 6 and 7, making them functions of the density of the concrete ρ through second degree polynomial expressions:

$$k_1(\rho) = -5.7378\cdot10^{-9}\rho^2 + 0.0003710\rho + 0.0866$$
$$k_2(\rho) = -1.1194\cdot10^{-7}\rho^2 + 0.0009045\rho + 0.8020$$
$$k_3(\rho) = -6.5941\cdot10^{-8}\rho^2 + 0.0003387\rho + 0.1999$$
$$k_4(\rho) = -3.5656\cdot10^{-7}\rho^2 + 0.0001801\rho - 1.4125$$

Figure 13 shows normalised failure envelopes in the axisymmetric stress plane and the corresponding complete failure surfaces in the three-dimensional stress space. Normalised results usually lead to strength data that tend to fall onto a single curve. This is a very convenient feature, since it allows the failure envelopes to be individually expressed as a function of f_c. However, as the density of the concrete decreases, the envelopes deviate toward the hydrostatic axis. So, to capture the behaviour of lightweight concretes, the effect of the increased porosity of the aggregates must be part of the failure criterion. To close the surfaces in tension, the tensile hydrostatic stress is limited to $0.05f_c$. As the figure shows, the shape of the failure surface in the deviatoric plane changes from almost triangular for low hydrostatic stresses to approximately circular with increasing hydrostatic pressure. This means that the state of stress at failure become less dependent on the rotational variable θ. This is probably due to the strength being limited by the compressibility of the aggregate. This is confirmed in Figure 14, where the failure envelopes are compared to strength data from a test programme in the octahedral stress plane [47]. This kind of representation shows that the compressive meridian and the tensile meridian of the failure surface generally do not coincide, with the tensile meridian normally being closer to the hydrostatic axis. This indicates that the strength of concrete is not merely a function of the state of stress at failure (σ_o; τ_o), but also depends on the load path taken to reach that particular combination of stresses. However, the envelopes tend toward a single curve as the hydrostatic stress component increases and the density of the concrete decreases.

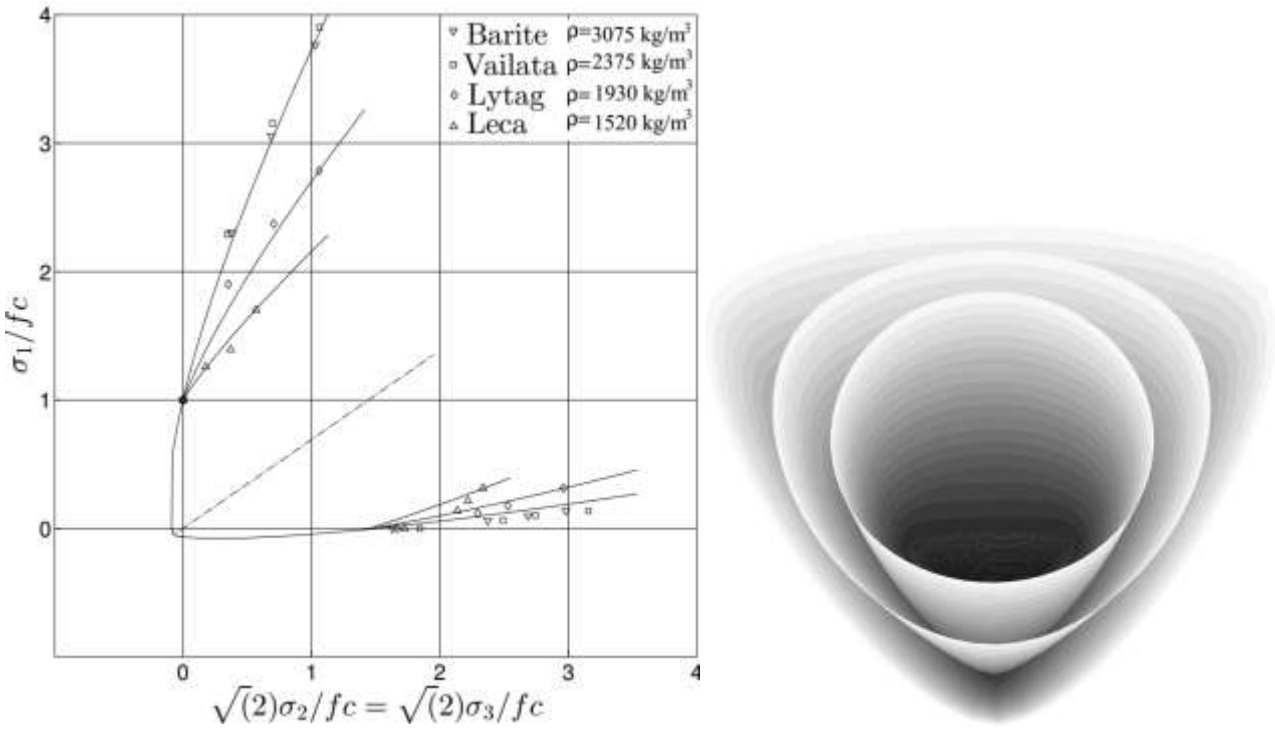

Fig. 13. Failure envelopes in the axisymmetric stress plane according to the proposed density-dependent octahedral expressions and the corresponding complete failure surfaces.

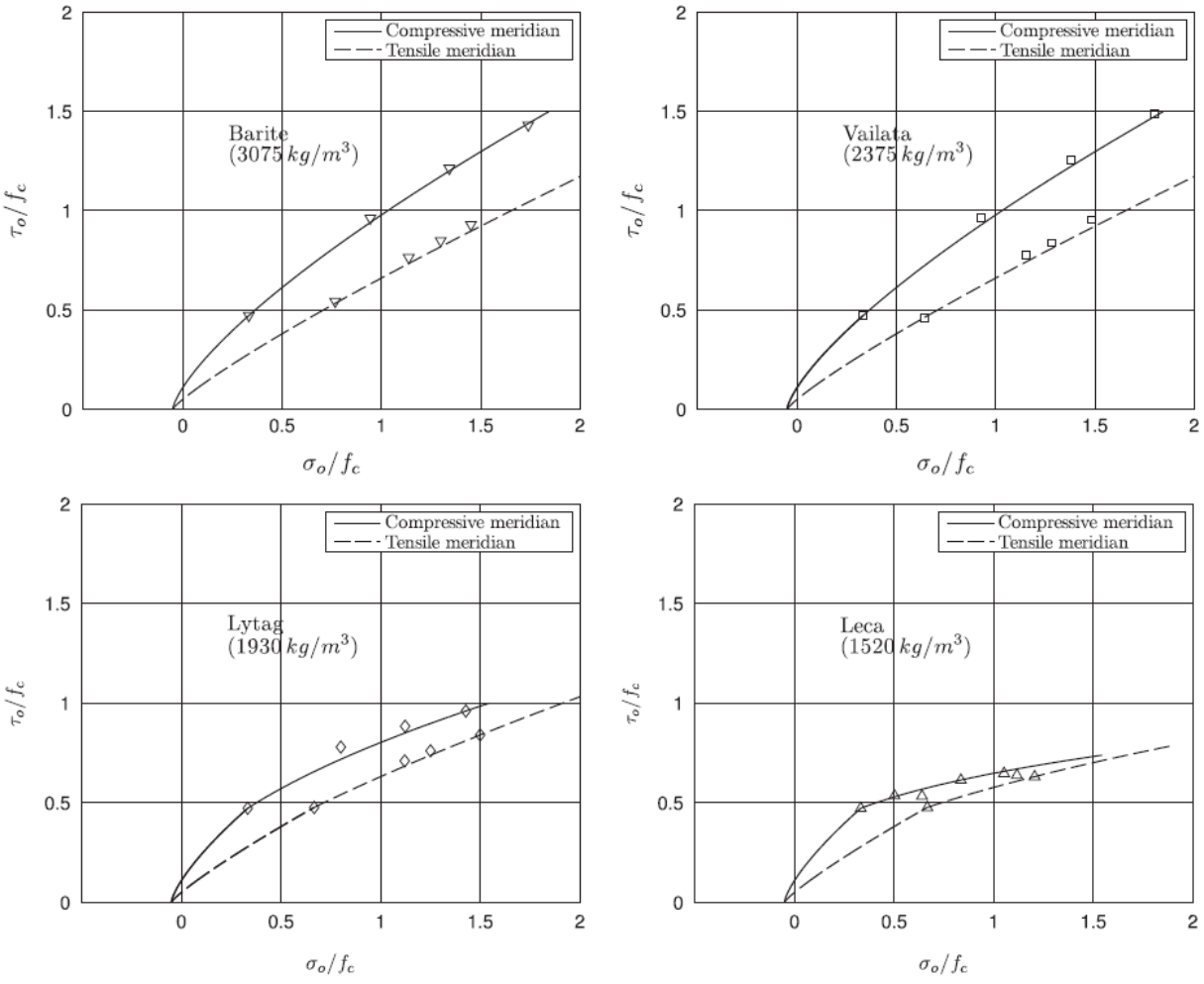

Fig. 14. Comparison of strength data with the proposed density-dependent failure criterion.

4.3 **Cracking**

Crack formation in the material model is represented by setting the modulus of elasticity to zero perpendicular to the crack plane and by reducing the shear modulus of the cracked Gauss point to a small value. This type of crack modelling, by altering the stiffness of the Gauss points, is referred to as smeared cracking, since the effect of cracking will be smeared over the entire region corresponding to the Gauss point for which the cracking criterion is exceeded. As argued in Section 3.3, the effect of aggregate interlock on the shear resistance is considered to be negligible. So, it would be more realistic to set the shear moduli of cracked concrete to zero. However, this would almost certainly lead to numerical instability in a brittle model. The shear modulus across the planes of the cracks was therefore defined by multiplying the uncracked values by a constant shear retention factor equal to 0.1. This value was considered to be large enough to promote stable numerical analyses, while at the same time being small enough to represent a nearly negligible effect from aggregate interlock on the load-carrying capacity.

5 Indications for triaxial failure and brittle material behaviour

The alleged difference in the ultimate limit state behaviour of NWC and LWAC structures is usually ascribed to the following features. Firstly, cracks tend to run through rather than around the aggregates in LWAC. This results in fewer contact points between the cracked surfaces and is therefore deemed to affect the forces that can be transferred across cracks through aggregate interlock. Secondly, the descending portion of the stress-strain curves in deformation-controlled tests is steeper for LWAC specimens than for NWC. Yet, despite these alleged differences in material behaviour, similar structural forms made of concretes with varying densities but the same compressive strength exhibit a similar or a nearly similar response. At least, this is the case in the upper density range for which most tests have been conducted. So, it seemed worth examining whether the working hypothesis in this research can better explain the seemingly surprising results. Three topics were picked out for further investigation: the shear resistance of beams with transverse reinforcement; the relationship between flexural and direct tensile strength; and the ductility of eccentrically loaded concrete prisms. The arguments are backed up by numerical results from nonlinear FE analyses using

the material model described in Section 4. It is important to emphasise that the concrete finite elements were never made smaller than 2-3 times the maximum size of the aggregate in the mix. This was because the material characteristics in the numerical model are derived from specimens which are sufficiently large to represent average properties of what is really a heterogeneous mix.

5.1 **Shear resistance of beams with transversal reinforcement**

In design codes, the assessment of shear resistance in concrete beams requiring transverse reinforcement has invariably been based on truss analogy. The diagonal struts are often allowed to rotate down to angles at ~20º. This small strut inclination activates a larger number of stirrups and therefore increases the shear resistance. The feasibility of the concrete struts rotating to such low angles depends on the redistribution capacity in the web and should therefore be a function of the effect of aggregate interlock and the steepness of the descending portion of the stress-strain curve in compression (or more precisely, in combined compression and tension). So, according to the variable strut inclination method, the rotational capacity of the concrete struts for beams made of LWAC would be expected to be significantly lower than that of their NWC counterparts. However, this does not accord with experimental results, where hardly any difference in behaviour is observed [37]. This has been explained by the irregular shape of the cracks in the lightweight members where, despite their broken aggregates, alternative contact points between the crack surfaces are considered to be able to develop. This might be a plausible explanation. However, if aggregate interlock is as important as it is claimed to be, at least some difference in behaviour would be expected to occur as a result of the distinct reduction in contact points between the crack surfaces. Furthermore, no explanation has been put forward to explain the lack of influence of the increased steepness of the descending portion of the stress-strain curve in compression.

In contrast, according to the hypothesis of this research, both the load-carrying capacity and the failure mechanism of an RC beam at its ultimate state are related to the region containing the compressive force path that develops due to bending, along which the applied load is also assumed to be transferred to the supports. So, the uncracked concrete in the compressive zone is considered to be the sole contributor to the shear resistance of the beam. The neglect of the effects of aggregate interlock and dowel action, which are

normally assumed to be vital for shear resistance, is deemed to be compensated for by the development of triaxial stress conditions in localised regions above deep cracks. This delays the development of tensile stresses caused by the shear forces. The degree of shear force required to cause failure in the compressive zone will therefore be significantly higher than that corresponding to the plane stress conditions that current design methodology assumes prevail in the beam. So, if the actual triaxial stress conditions that inevitably develop at the ultimate limit state are taken into account, it can be argued that the uncracked concrete in the compressive zone is able to sustain both the compressive force from bending and the total shear force, even though the depth of this zone may become very small. Failure of the beam should therefore be expected to be associated with the stress conditions in the region of the path along which the compressive force is transferred to the supports.

As explained in Section 3.1, failure of RC members has invariably been found to be caused by the development of tensile stresses in the region of the CFP. The reason for adding additional reinforcement to the beam is therefore to help the concrete combat these stresses. The aim of the design is to delay the failure of the CFP until the flexural reinforcement has been allowed to yield. LWAC members in the normal strength and density range should not be expected to display any marked differences in shear behaviour, because the strength in compression-tension-tension is likely to become the controlling factor and only small differences are expected here. So, although the degree of stress triaxiality and the triaxial compressive strength is considered to be lower for LWAC, these effects are not considered to be serious enough to turn the highly stressed compressive regions above deep cracks into the critical ones. This is a direct result of concrete's extreme sensitivity to tensile stresses. However, one should be aware that this might change for mixes close to or at the ceiling strength.

To support the hypothesis in this research, numerical analyses were carried out on beams taken from a test programme conducted by Walraven and Al-Zubi [37]. The aim of their test programme was to investigate whether the variable strut inclination method could also be applied with LWAC members. The beams were subjected to four-point bending with a free span of 5m, and the distance between the point loads was 1.6m. The beams analysed were reinforced by 6φ25 in two layers as tensile reinforcement, φ10 with spacing

108mm as transverse reinforcement, and 6φ12 as compressive reinforcement. The dimensions of the cross-section and finite element model are given in Figure 15. Only a quarter of the beams were modelled with three-dimensional brick elements, due to the relevant symmetries. During testing all beams were considered to fail by crushing of the web before the yield strain of the flexural reinforcement was attained.

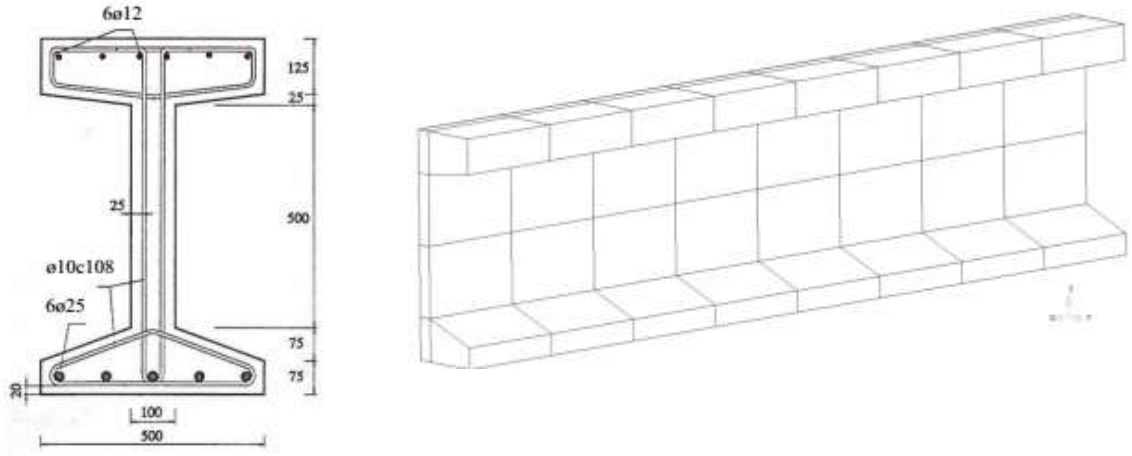

Fig. 15. Cross-section of beam and FE model.

Table 1 presents the experimental and numerical results for the beams with different types of aggregate. The main aim of the numerical study was to investigate whether the beams could carry the applied load without the aid of aggregate interlock, strain-softening, and dowel action. This seems to be possible, since the experimental and numerical results nearly coincide even though these effects were neglected in the analyses. Furthermore, the crack patterns in Figure 16 for the mid-breadth plane of the beam with Lytag as aggregate show that the structural collapse was triggered by the vertical splitting of the previously uncracked concrete in the compressive zone. A stabilised crack pattern developed at approximately 50% of the failure load. This means that it was the development of secondary tensile stresses in the compressive zone that was responsible for the failure. The failure criterion under fully compressive stress states was the only factor that varied with the density of the concrete, so the only input parameter governing the numerical response was the uniaxial cylinder strength. This is consistent with the experimental results in Table 1, where the ultimate load-carrying capacity seems to be merely a function the strength of the concrete.

Table 1:

Experimental and numerical results

Aggregate type	Density (kg/m^3)	f_{cube} (MPa)	f_{split} (MPa)	P_{exp} (kN)	P_{num} (kN)	P_{exp}/P_{num}
Gravel	2370	30.9	2.46	470	490	0.96
Aerdelite	2095	25.3	1.95	482	410	1.18
Lytag	1938	31.5	2.43	481	490	0.98
Liapor	1728	31.5	2.43	541	590	0.92

It was claimed above that it is the splitting of the compressive flange that most likely leads to the failure of the beams. The crushing of the web must then be a post-failure phenomenon, caused by the loss of strength and stiffness previously provided by the flange. If this is true, the main task of the designer should be to prevent the compressive flange from collapsing before the flexural reinforcement has been allowed to yield. In this respect, hoop-flange reinforcement was found to play an important role, since it delayed the occurrence of the vertical splitting cracks. As a final remark, it should be emphasised that the numerical analyses are not considered to provide an absolute proof for the above claim. For this, experimental tests especially tailored to the above numerical findings will be needed.

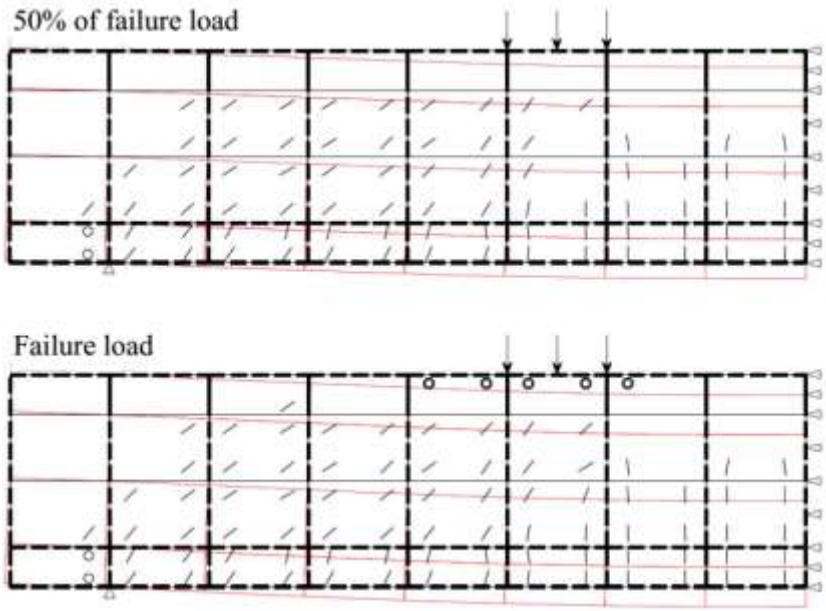

Fig. 16. Crack pattern and deflected geometry for a beam with Lytag in the numerical study.

5.2 **Relationship between flexural and direct tensile strength**

The flexural tensile strength of concrete is greater than its direct tensile strength. This has frequently been attributed to a gradual loss of load-carrying capacity of the concrete at the material level when the direct tensile strength at the most stressed fibre has been exceeded [48]. According to this model, the relationship between flexural and direct tensile strength should depend on the brittleness of the concrete over a characteristic length given by the expression:

$$l_{ch} = \frac{G_F \cdot E}{f_t^2} \tag{8}$$

where G_F is the fracture energy consumed during formation of a true stress free crack, E is the dynamic modulus of elasticity, and f_t is the direct tensile strength. The fracture energy is associated with the area under the descending portion of the stress-strain curve in tension. So, LWAC or high-strength NWC, which tend to fail in a brittle manner, should be expected to have a low flexural-to-direct-tensile-strength ratio. However, experimental tests have shown that these concretes, despite their considerably smaller characteristic lengths, exhibit similar or even higher flexural-to-direct tensile-strength ratios than those of ordinary concretes [49]. This has been related to differences in the general shape of the descending branch of the stress-strain curves in tension. According to these curves, a greater part of the fracture energy is consumed at smaller crack widths for LWAC than for NWC. Since the stress transfer at small crack widths is considered to be the main contributor to the overall stress redistribution capacity of the concrete in a structure, this has been accepted as an adequate explanation for what at first sight seemed like contradictory experimental and theoretical results.

However, it does not seem necessary to invoke the notion of tensile strain-softening to explain why the flexural tensile strength is greater than the direct tensile strength. When a plain concrete member is simply loaded with a transverse load until it breaks, the initiation of cracking at the extreme tensile fibre immediately leads to the failure of the specimen. So the fact that the flexural tensile strength corresponding to the breaking load tends to be higher than the direct tensile strength can be explained by the weakest link theory. Localised weaknesses inevitably develop in a heterogeneous material like concrete. In a three-point bend test only the extreme fibres in the cross section beneath the point load are at the greatest stress, while in a direct tensile test all fibres are at the same stress and failure will be initiated when the weakest fibre reaches

its limiting tensile stress. Furthermore, this statistical size effect also explains the approx. 20% lower flexural strength found in four-point beam bending tests than in three-point beam bending tests, since in the former all cross sections between the point loads will be critical. Moreover, the high degree of brittleness in concrete is connected with a minimum amount of microcracking within the material. The result is a more linear stress-strain behaviour, which tends to move the resultant of the internal actions closer to the extreme fibres and therefore increases the beam's bending resistance. So it is not surprising that the flexural-to-direct-tensile-strength ratio for concretes suffering highly brittle failures increases rather than decreases as predicted by the tensile strain-softening models.

The purpose of the kind of three-point bend test depicted in Figure 17 is to measure the amount of energy absorbed in the fracture zone when the beam is broken into two halves [50]. This energy is further divided by the fracture area to obtain the fracture energy. This is a fracture mechanics parameter which is deemed to describe the ability of concrete to resist cracking. An inverse analysis must then be performed to obtain the descending portion of the uniaxial stress-strain curve in tension for use in numerical analyses.

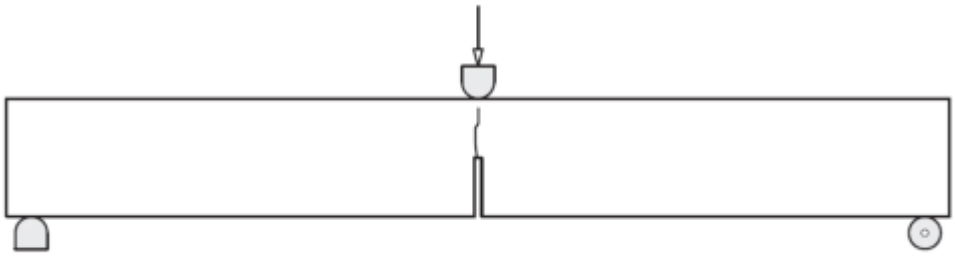

Fig. 17. Three-point bend test in a notched beam.

Alternatively, the fracture energy G_F and the descending portion of the stress-strain curve can be obtained directly from uniaxial tensile tests. However, it is very difficult to control the fracture in these tests, since the stiffness of the testing machine must at all times be greater than the steepest slope of the descending branch [51]. This is a very strict requirement that is unlikely to hold for concrete in a structure. The same argument can therefore be applied to the three-point bend test, since this is only an easier way of creating the stiff

testing environment needed to control the fracture (the large deflection of the beams makes it easy to obtain stable tests for testing machines that use position control).

Regardless of the above reasoning, there is also another feature calling into question the possibility of considering G_F a material property: the fracture energy obtained with the procedure proposed by RILEM TC-50 sometimes increases by more than 50% when the size of the specimen is increased three times [52]. This can either be an artefact of the test method or an intrinsic size effect of G_F. If the latter is true, the fracture energy cannot be considered a material property. Guinea, Planas and Elices [53-55] set out to systematically explore all possible sources of energy dissipation, apart from that of the fracture itself, which were not taken into account by the RILEM recommendation. They found several size-dependent sources of energy dissipation (non-ideal boundary conditions, energy dissipation in the bulk of the specimen, etc.), and they estimated the corresponding dissipated energy. After taking into account the estimated energy corrections, 32% was still missing from any real-size independent G_F value. However, they showed that if the energy corresponding to the tail of the load-deflection curve was taken into account, an almost constant G_F value was obtained regardless of the size of the specimen. This saved the fracture energy parameter as a material property and improved confidence in modelling concrete as a cohesive material.

The tail of the load deflection curve cannot be measured in the RILEM tests, because, to keep things simple, the effect of the weight of the beam on fracture is not compensated for. Instead, the tests are stopped at a certain stage and the remaining dissipated energy neglected. Alternatively, the weight of the beam can be compensated for and the tests controlled up to absolute breakage of the specimen. In the last part of such tests, the crack penetrates very deeply into the compressive zone. Despite this, the beam can still carry the decreasing load. This is normally attributed to further resistance in the opening of the crack. However, at this advanced stage of cracking, it seems more likely that the specimen carries the load by arch action. The compressive zone is able to sustain high compressive stresses due to the triaxial stress condition that develops in the highly-stressed region above the deep crack. Moreover, it has been demonstrated that, although the friction in the rolling support is not high for most of the test, it becomes very high for small normal loads [54]. So, in the late stage of bending, the conditions are very well-suited for the specimen to

carry the load as a three-hinged arch. If this is the case, the tail of the load-deflection curve cannot be used to save fracture energy as a material parameter.

To demonstrate the possible arch effect, a simple illustrative numerical analysis was carried out for a 100x100x800mm plain concrete beam with f_c = 25MPa. The supports were restrained and the beam was loaded at mid-span in steps of 1kN until failure. This analysis should not be seen as an attempt to simulate an actual three-point bend test, but merely as a demonstration of a plain concrete beam's ability to carry a transverse load by arch action if sufficient lateral restraint is able to develop. The main result from the analysis is presented in Figure 18. The red and blue orientated lines are the maximum principal tensile and compressive stresses respectively, while the black orientated lines represent the cracks. The first flexural crack occurs at 2kN and extends in the next load step. From this stage on, however, the crack does not propagate any further into the beam. This is because the load is transferred directly to the supports by a straight thrust line and it is very hard for the crack to progress into the triaxially confined compressive zone. In load step 10, the dilation of the highly-stressed region has induced large tensile stresses in the adjacent concrete, which cause the beam to fail in the next load step. The results demonstrate that the specimen is fully capable of behaving like a three-hinged arch as long as the necessary lateral restraint can be provided by friction. Since the highly-stressed region above the crack is not likely to fail, the specimen will be able to carry the external load by arch action even if the compressive zone is very small.

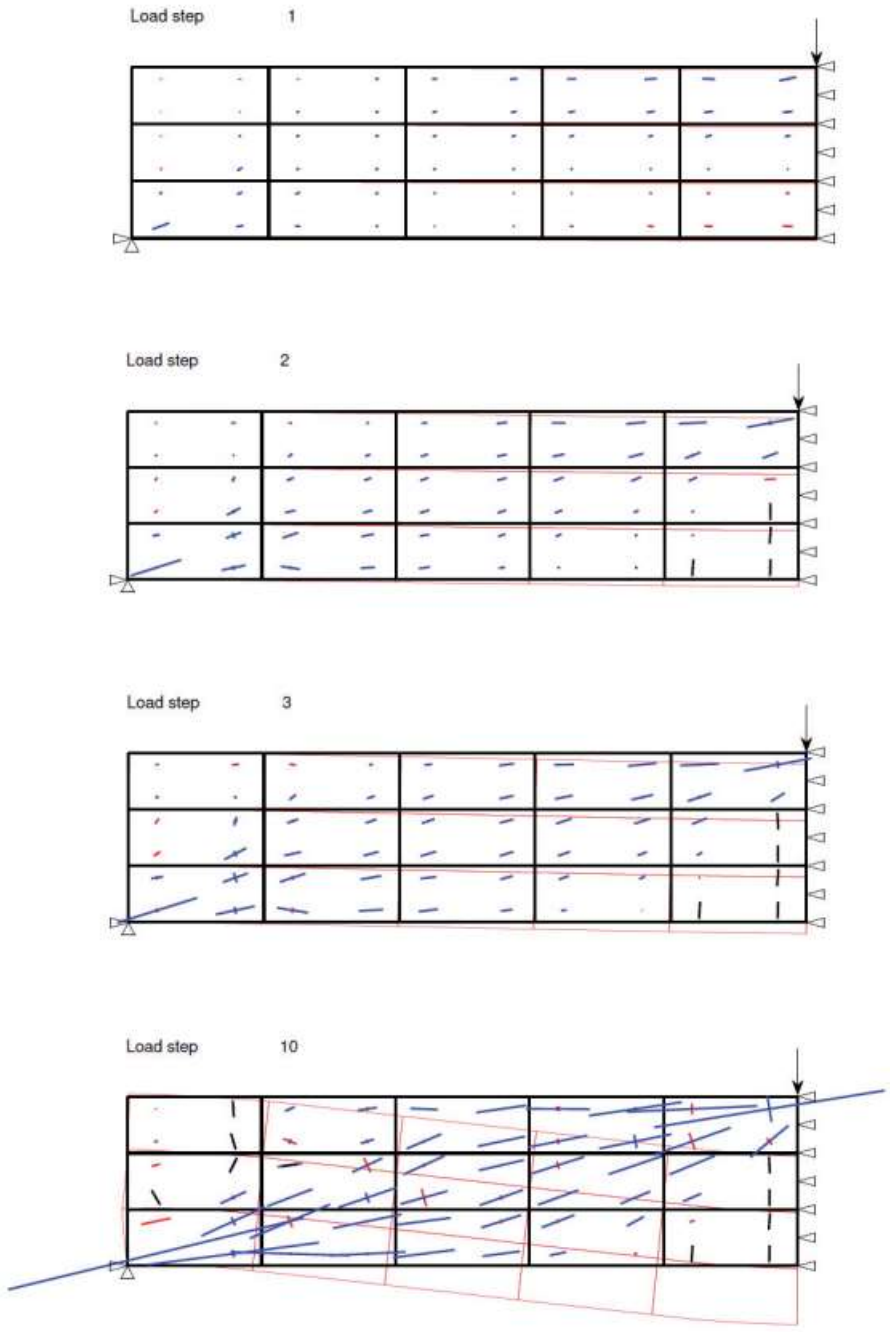

Fig. 18. Principal stresses and crack pattern in a plain concrete beam.

5.3 **Eccentrically loaded concrete specimens**

The compressive strain in the extreme fibre of plain concrete prisms increases with an increasing degree of eccentricity in loading. This increase in ductility is commonly believed to be related to an upward shift of the

descending branch of the stress-strain curve in compression for increasing strain gradients. This research did not cover compressive strain-softening characteristics at the material level, but relies on the triaxiality of the compression zone of the structure, which governs its overall strength and ductility. LWAC members are expected to exhibit fewer triaxial effects near failure than NWC members and will therefore tend to behave in a more brittle manner. A good measure for the expected triaxiality and therefore ductility of the concrete is given by the percentage of inelastic to elastic strain at failure.

$$D = \frac{\varepsilon_{cu} - \varepsilon_{el}}{\varepsilon_{el}} \cdot 100\% \tag{9}$$

where ε_{cu} is the compressive strain in the concrete at peak stress and ε_{el} is the elastic part of the strain. The D-ratio describes how much the stress-strain curve deviates from linearity and reflects the extent of microcracking within the material before the peak load level is attained. Microcracking is known to influence concrete behaviour positively, by reducing the likelihood of sudden failures caused by splitting along steel bars or spalling of concrete cover. Moreover, it determines the triaxiality of the member and therefore its ductility.

The results of an experimental programme conducted by Markeset and Hansen were used to investigate the above hypothesis [49]. Table 2 gives the maximum sustained load and the corresponding compressive strain in the extreme fibre for plain 125x175x600mm rectangular concrete prisms with an increasing degree of eccentricity in loading (*e/h* = 0/0.056/0.167), see Figure 19. The aim of the experimental programme was to investigate how material brittleness affects structural ductility. Concrete mixes with varying brittleness as defined by their characteristic lengths were obtained by using various types of aggregates and cement and silica contents. Special concern was attached to the behaviour of the LWACs, which were expected to exhibit highly brittle structural behaviour in accordance with their characteristic length brittleness measure, which is related to the post-peak stress-strain characteristics of the concrete. However, as has been repeatedly demonstrated in this chapter, there are again no dramatic differences between NWC and LWAC structures, despite the latter's poor post-peak behaviour at the material level.

Table 2:

Experimental and numerical results

Aggregate type	Density (kg/m^3)	f_c (MPa)	E_c (GPa)	e/h	P_{exp} (kN)	$\varepsilon_{c,max}$ (‰)	P_{num} (kN)	P_{exp}/P_{num}	D (%)
Liapor 8	2040	86.8	30.5	0	1900	3.12	1881	1.01	9.6
				0.056	1580	3.41	1477	1.07	
				0.167	1136	3.55	1028	1.11	
Gneiss	2470	81.4	35.7	0	1780	2.61	1722	1.00	14.5
				0.056	1518	2.97	1411	1.08	
				0.167	1108	3.16	984	1.13	
Basalt	2570	89.0	43.1	0	1947	2.72	1947	1.00	31.7
				0.056	1674	3.31	1509	1.11	
				0.167	1228	3.45	1050	1.17	
Quartzite	2442	86.5	40.2	0	1892	2.47	1881	1.01	14.8
				0.056	1640	2.81	1477	1.11	
				0.167	1132	2.84	1017	1.11	

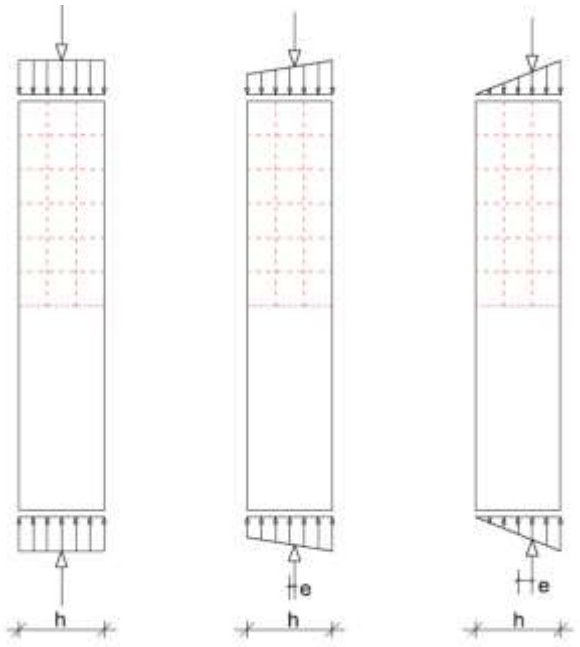

Fig. 19. Idealised stress distribution and finite element mesh for the three load cases.

The results given in Figure 20 show that there are almost no differences in the relative decrease in strength at failure for the various mixes. On the other hand, there is a mild difference in the relative increase in strain, this being greatest for the Basalt concrete, somewhat less for the Gneiss/granite and Quartzite concrete, and slightly lower again for the Liapor concrete. However, this is just what should be expected from the D-ratios, which express the expected triaxiality and therefor ductility in the structure. By simply multiplying the

concentric strain at failure by a factor corresponding to the D-ratio, strain values equal to 3.42, 2.99, 3.58 and 2.83‰ are obtained for the various concretes, which corresponds surprisingly well with the observed eccentric strains.

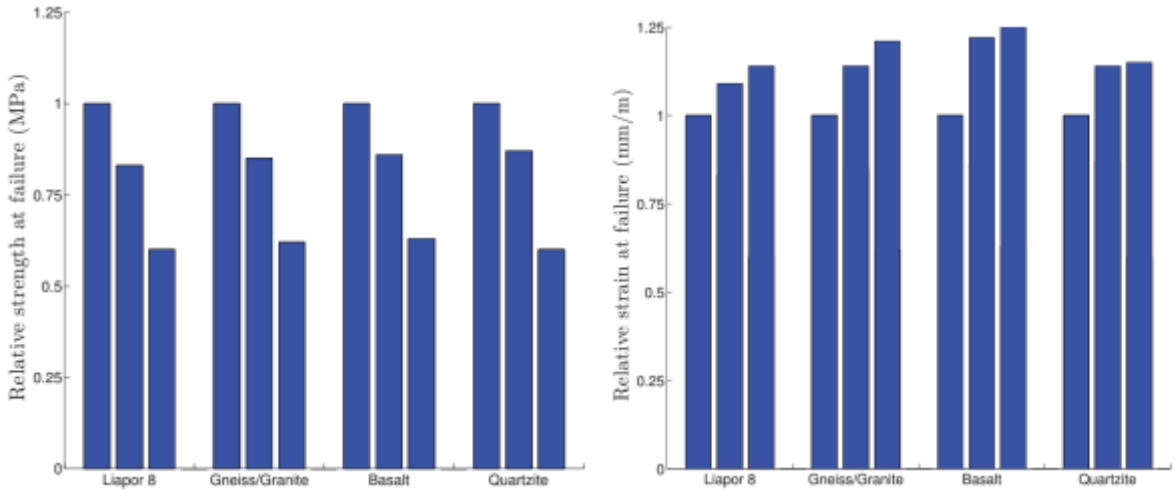

Fig. 20. Decrease in relative strength and increase in relative strain at failure.

Table 2 compares numerical results from plane stress analyses with the maximum loads obtained in the experimental test program. The eccentrically loaded prisms failed due to vertical cracks that initiated in the most stressed corner, see Figure 21. The numerical results agree with the experimental results. The somewhat lower maximum sustained loads in the analyses may be because the prisms were subjected to an applied load in the analyses, but an applied displacement in the experiments. It is interesting to note that eccentrically loaded prisms tend to collapse due to a flexural failure in their central zone in a manner akin to that of RC beams. So, the same arguments used to explain the structural ductility of RC beams in flexure can be used to explain the large strains measured on the compressive face of plain concrete prisms under eccentric loading.

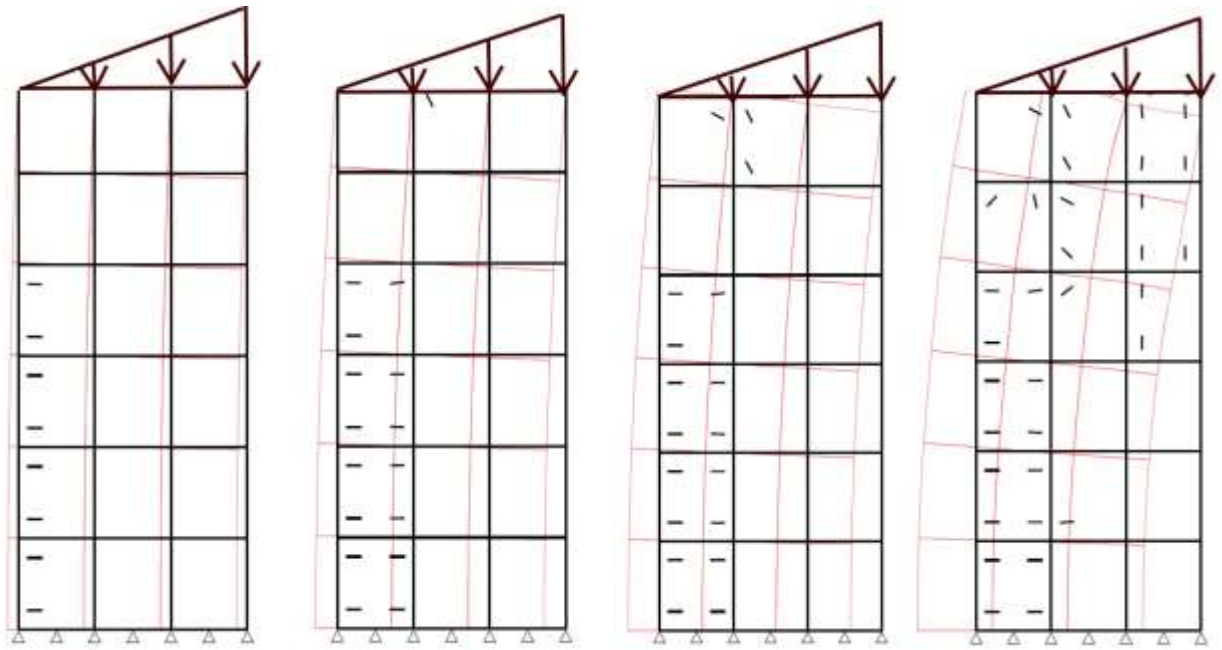

Fig. 21. Typical development of crack pattern and deformed shape for eccentrically loaded prisms.

6 Conclusions

The main hypothesis of this research was that the key material features that generally dictate concrete structural behaviour in the ultimate limit state are:

1. The large effect small secondary stresses have on the strength of concrete: compressive stresses increase the load-carrying capacity in the main direction considerably, while tensile stresses have a dramatic opposite effect.
2. The abrupt increase of the transverse expansion of concrete at a stage close to the peak stress level, i.e. the rapid increase of Poisson's ratio as failure is approached.
3. The rapid unloading of concrete beyond the peak stress level, i.e. the brittle fracture of concrete at the material level.

It follows from these features that the ductility of structural members arises from local triaxial stress conditions that develop within the compressive zone prior to failure rather than from stress-redistributions due to a gradual decay of load-carrying capacity at the material level, as is commonly believed. The higher the triaxial stress at a critical cross-section, the larger the corresponding strains and the larger the resulting

ductility of the structure. Since these stresses develop just prior to failure, it is mainly the ductility that will be affected, not so much the maximum load-carrying capacity of the member.

This means that the difference between NWC and LWAC should not be sought in the post-peak material characteristics, as is the usual line of action, but rather in the degree of stress triaxiality in the compressive zone. This explains why the ductility of LWAC members tends to decrease somewhat (owing to a smaller degree of stress triaxility in the member as a result of a smaller transverse expansion of the concrete prior to failure which is linked to a limited degree of microcracking within the material), while the load-carrying capacity is often similar to that of corresponding NWC members. When characterising different concretes it is important to realise that the type of aggregate has a large influence upon the bond between aggregate and mortar and plays an important role in the distribution of the internal stresses in the concrete. In some cases, this factor is more important than the density of the aggregate.

Acknowledgements

Most of this paper is based on the PhD thesis of Håvard Nedrelid from the Norwegian University of Science and Technology. Sadly, he passed away in 2015. In his memory, the author hopes he has been able to present the research with the respect and quality it deserves. The work was carried out with financial support from COIN, the Concrete Innovation Centre, which was a centre for research-based innovation with funding from the Research Council of Norway and industrial partners in the period 2006-2014.

References

[1] ACI Committee 213. Guide for Structural Lightweight Aggregate Concrete (ACI 213R-03). American Concrete Institute. Farmington Hills, MI, United States: American Concrete Institute; 2003.
[2] fib bulletin 8. Lightweight Aggregate Concrete. Lausanne, Switzerland: International federation for Structural Concrete; 2000.
[3] Ingebrigtsen T. Stolma Bridge, Norway. Structural Engineering International. 1999;9:100-2.
[4] Melby K. Use of high strength LWAC in Norwegian bridges. In: Helland S, editor. International Symposium on Structural Lightweight Aggregate Concrete. Kristiansand, Norway: Norwegian Concrete Association; 2000.
[5] Haug AK, Fjeld S. A floating concrete platform hull made of lightweight aggregate concrete. Engineering Structures. 1996;18:831-6.

[6] fib Bulletin 45. Practitioner's guide to finite element modelling of reinforced concrete structures. In: Foster S, Maekawa F, Vecchio F, editors. Lausanne, Switzerland: International Federation for Structural Concrete (fib); 2008.
[7] Collins MP, Vecchio FJ, Mehlhorn G. An international competition to predict the response of reinforced concrete panels. Canadian Journal of Civil Engineering. 1985;12:624-44.
[8] Jaeger T, Marti P. Reinforced Concrete Slab Shear Prediction Competition: Entries and Discussion. ACI Struct J.106.
[9] Vidosa FG, Kotsovos MD, Pavlović MN. Nonlinear finite-element analysis of concrete structures: Performance of a fully three-dimensional brittle model. Computers & Structures. 1991;40:1287-306.
[10] Øverli JA, Jensen TM. Increasing ductility in heavily reinforced LWAC structures. Engineering Structures. 2014;62–63:11-22.
[11] Vázquez-Herrero C, Martínez-Lage I, Vázquez-Vázquez H, Martínez-Abella F. Comparative study of the flexural behavior of lightweight and normal weight prestressed concrete beams. Engineering Structures. 2013;56:1868-79.
[12] Carmo RNF, Dias-da-Costa D. Tensile and flexural behaviour of LWAC members under short-term service loads. Engineering Structures. 2015;92:142-55.
[13] Dias-da-Costa D, Carmo RNF, Graça-e-Costa R, Valença J, Alfaiate J. Longitudinal reinforcement ratio in lightweight aggregate concrete beams. Engineering Structures. 2014;81:219-29.
[14] Nedrelid H. Towards a better understanding of the ultimate behaviour of lightweight aggregate concrete in compression and bending. Trondheim: Norwegian University of Science and Technology; 2012.
[15] Holand I, Hammer TA, Fluge Fe. International Symposium on Structural Lightweight Aggregate Concrete: Proceedings, Sandefjord, Norway. Oslo: Norwegian Concrete Association; 1995.
[16] Kotsovos MD, Pavlović MN. Structural concrete: Finite-element analysis for limit-state design. London: Thomas Telford Ltd; 1995.
[17] Engen M, Hendriks MAN, Øverli JA, Åldstedt E. Solution strategy for non-linear finite element analyses of large reinforced concrete structures. Struct Conc. 2015;16:389-97.
[18] Hansen TC. Swedish Cement and Concrete Research Institute. 1958;29.
[19] Bardhan-Roy BK, Crozier WFG, (Eds). FIP manual of lightweight aggregate concrete: Glasgow : Surrey University Press; 1983.
[20] RILEM TC 148-SSC. Test method for measurement of the strain-softening behaviour of concrete under uniaxial compression. Materials and Structures. 2000;33:347-51.
[21] Standards Norway. NS-EN 1992-1-1:2004+NA:2008. Eurocode 2: Design of concrete structures - Part 1-1: General rules and rules for buildings. Norway: Standards Norway; 2008.
[22] van Mier JGM, Shah SP, Arnaud M, Balayssac JP, Bascoul A, Choi S et al. Strain-softening of concrete in uniaxial compression. Materials and Structures. 1997;30:195-209.
[23] Kotsovos MD. Effect of testing techniques on the post-ultimate behaviour of concrete in compression. Matériaux et Construction. 1983;16:3-12.
[24] Mander J, Priestley M, Park R. Theoretical Stress-Strain Model for Confined Concrete. J Struct Eng. 1988;114:1804-26.
[25] Attard MM, Setunge S. Stress-strain relationship of confined and unconfined concrete. ACI Materials Journal. 1996;93:432-42.
[26] Mander JB, Priestley MJN, Park R. Observed stress-strain behavior of confined concrete. J Struct Eng. 1988;114:1827-49.
[27] Gerstle KH, Linse DL, Bertacchi P, Kotsovos MD, Ko H-Y, Newman JB et al. Strength of Concrete under Multiaxial Stress States. ACI - Special Publication. 1978;SP-55:103-31.
[28] Smith SS, Willam KJ, Gerstle KH, Stein S. Concrete Over the Top--Or, is there Life After Peak? Materials Journal. 1989;86:491-7.
[29] Gerstle KB, Zimmerman RM, Winkler H, Traina LA, Taylor MA, Schickert G et al. Behavior of Concrete under Multiaxial Stress States. Journal of the Engineering Mechanics Division. 1980;106:1383-403.
[30] Kotsovos MD, Pavlović MN. Ultimate limit-state design of concrete structures: A new approach. London: Thomas Telford Ltd; 1999.
[31] Ferguson PM. Discussion of "Diagonal tension in reinforced concrete beams" by A.P. Clark. ACI Journal. 1952;48:156-1 to -3.
[32] Kotsovos MD. Compressive Force Path Concept: Basis for Reinforced Concrete Ultimate Limit State Design. ACI Struct J. 1988;85:68-75.

[33] Markeset G. Failure of concrete under compressive strain gradients. Trondheim: Department of Structural Engineering, Norwegian Institute of Technology, University of Trondheim, Norway; 1993.
[34] Fenwick RC, Paulay T. Mechanisms of shear resistance of concrete beams. ASCE Journal of the Structural Division. 1968;94:2325-50.
[35] Reinhardt HW, Walraven JC. Cracks in concrete subject to shear. ASCE Journal of the Structural Division. 1982;108:207-24.
[36] Kotsovos MD, Bobrowski J, Eibl J. Behaviour of Reinforced Concrete T-Beams in Shear. The Structural Engineer. 1987;65B(1):68-75.
[37] Walraven J, Al-Zubi N. Shear capacity of lightweight concrete beams with shear reinforcement. In: Holand I, Hammer T, Fluge F, editors. International Symposium on Structural Lightweight-Aggregate Concrete. Sandefjord, Norway: Norwegian Concrete Association; 1995. p. 91-104.
[38] Jelić I, Pavlović MN, Kotsovos MD. A study of dowel action in reinforced concrete beams. Magazine of Concrete Research. 1999;51:131-41.
[39] Thorenfeldt E, Stemland H. Shear capacity of lighweight concrete beams without shear reinforcement. In: Holand I, Hammer T, Fluge F, editors. International Symposium on Structural Lightweight-Aggregate Concrete. Sandefjord, Norway: Norwegian Concrete Association; 1995. p. 244-55.
[40] Thorenfeldt E, Stemland H. Shear capacity of lighweight concrete beams without shear reinforcement. In: Helland S, Holand I, Smeplass S, editors. Second International Symposium on Structural Lightweight-Aggregate Concrete. Kristiansand, Norway: Norwegian concrete Association; 2000. p. 330-41.
[41] Kani MW, Huggins MW, Wiltkopp RR. Kani on shear in reinforced concrete. Canada: Department of Civil Engineering, University of Toronto; 1979.
[42] Kotsovos MD. A mathematical model of the deformational behavior of concrete under generalised stress based on fundamental material properties. Matériaux et Construction. 1980;13:289-98.
[43] Markou G, Papdrakakis M. Computationally efficient 3D finite element modeling of RC structures. Computers and Concrete. 2013;12:443-98.
[44] Kotsovos MD. Concrete. A brittle fracturing material. Matériaux et Construction. 1984;17:107.
[45] Willam KJ, Warnke EP. Constitutive model for the triaxial behaviour of concrete. Proceedings Colloquium on Concrete Structures Subjected to Triaxial Stresses, IABSE Report 19. Zurich: IABSE; 1974.
[46] Øverli JA. A density-dependent failure criterion for concrete. Construction and Building Materials. 2016;124:566-74.
[47] Berra M, Fatticciono A, Ferrara G. Triaxial behaviour of concretes of different weight. RILEM International Conference on Concrete under Multiaxial Conditions. Toulouse, France: Presses de'l Universite Paul Sabatier; 1984. p. 176–89.
[48] Hillerborg A, Modéer M, Petersson PE. Analysis of crack formation and crack growth in concrete by means of fracture mechanics and finite elements. Cement and Concrete Research. 1976;6:773-81.
[49] Markeset G, Hasnsen EA. Brittleness of high strength LWA concrete. In: Holand I, Hammer T, Fluge F, editors. International Symposium on Structural Lightweight-Aggregate Concrete. Sandefjord, Norway: Norwegian Concrete Association; 1995. p. 220-31.
[50] Hillerborg A. The theoretical basis of a method to determine the fracture energy G_F of concrete. Materials and Structures. 1985;18:291-6.
[51] Barnard PR. Researches into the complete stress-strain curve for concrete. Magazine of Concrete Research. 1964;16:203-10.
[52] Hillerborg A. Results of three comparative test series for determining the fracture energy G_F of concrete. Materials and Structures. 1985;18:407-13.
[53] Guinea GV, Planas J, Elices M. Measurement of the fracture energy using three-point bend tests: Part 1—Influence of experimental procedures. Materials and Structures. 1992;25:212-8.
[54] Planas J, Elices M, Guinea GV. Measurement of the fracture energy using three-point bend tests: Part 2—Influence of bulk energy dissipation. Materials and Structures. 1992;25:305-12.
[55] Elices M, Guinea GV, Planas J. Measurement of the fracture energy using three-point bend tests: Part 3—influence of cutting theP-δ tail. Materials and Structures. 1992;25:327-34.

Figure captions